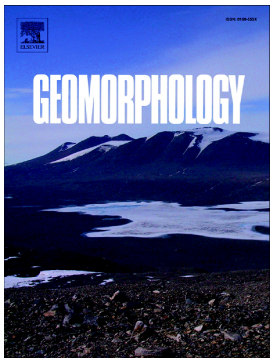

Application of the Schmidt-hammer for relative-age dating of glacial and periglacial landforms in the Cantabrian Mountains (NW Spain)

Javier Santos-González, R.B. González-Gutiérrez, A. Gómez-Villar, S.A. Peña-Pérez, A. Melón-Nava, A. Pisabarro, J.M. Redondo-Vega

PII: S0169-555X(24)00160-0

DOI: https://doi.org/10.1016/j.geomorph.2024.109210

Reference: GEOMOR 109210

To appear in: *Geomorphology*

Received date: 13 October 2023

Revised date: 11 April 2024

Accepted date: 12 April 2024

Please cite this article as: J. Santos-González, R.B. González-Gutiérrez, A. Gómez-Villar, et al., Application of the Schmidt-hammer for relative-age dating of glacial and periglacial landforms in the Cantabrian Mountains (NW Spain), *Geomorphology* (2023), https://doi.org/10.1016/j.geomorph.2024.109210

Application of the Schmidt-hammer for relative-age dating of glacial and periglacial landforms in the Cantabrian Mountains (NW Spain)

Javier Santos-González[1*], R.B. González-Gutiérrez[1], A. Gómez-Villar[1], S.A. Peña-Pérez[1], A. Melón-Nava[1], A. Pisabarro[1], J.M. Redondo-Vega[1]

[1] Department of Geography and Geology, Universidad de León. Campus de Vegazana, s/n. 24071 León (Spain)

[*]Corresponding author e-mail: jsango@unileon.es

Abstract

A Schmidt hammer was applied for relative-age dating to 48 sites in 5 different massifs of the Cantabrian Mountains (NW Spain). The sample included glacial (moraines, erratics, and polished bedrock) and periglacial (rock glaciers, blockfields, and talus slopes) sites from the last glaciation to the present in different geomorphological contexts. The rebound (R) values agree with the morphostratigraphic reconstructions, showing progressively lower values for older deposits. Six stages from the Last Glacial Maximum to the present are inferred. The results differ according to the lithology: i) the quartzites showed higher R-values and very low weathering rates; ii) the granodiorites showed larger differences in R-values reflecting clearly age differences; iii) sandstones appear to be unsuitable for Schmidt hammer measurements in some areas; however, quartzite sandstones provide better results. The rock glaciers formed in different periods after deglaciation (i.e. just after the Last Glacial Maximum, Bölling/Allerød, Holocene), indicate a paraglacial dependence rather than climate-driven landforms. The sampled

blockfields stabilized after the (almost) total deglaciation of the cirques, but their origin and significance in this mountainous area remain poorly understood.

Key words: Schmidt hammer; Deglaciation; Rock glaciers; Blockfields; Cantabrian Mountains

1. Introduction

A Schmidt hammer is an instrument that measure the uniaxial compressive strength (in MPa/Nmm^2) of a surface, giving a rebound (R) value between 0 and 100 that could be used to assess rock hardness. Exposed rock surfaces progressively exhibit lower R-values as weathering increases, allowing these values to be used for relative age dating (Goudie, 2006). The use of Schmidt hammer in geomorphology has increased in recent years and detailed descriptions about different types and applications could be found in the work of Matthews and Winkler (2022).

Specifically, the Schmidt hammer has been used to reconstruct glacier evolution and deglaciation, mainly from the Holocene (Evans et al., 1999; Winkler et al., 2003; Winkler, 2005; Shakesby et al., 2004, 2006, 2011; Ffoulkes and Harrison, 2014; Matthews et al., 2014; Tanarro et al., 2021), but also from the Younger Dryas (Anderson et al., 1998; Ballantyne, 1997; Hughes et al., 2019; Matthews et al., 2023) or from earlier in the Last Glacial Period (McCarroll and Nesje, 1993; Rae et al., 2004; Engel, 2007; Černá and Engel, 2011; Kłapyta, 2013; Tomkins et al., 2016, 2018b, 2018a; de Marcos et al., 2022; Tonkin, 2022). For granite surfaces, the maximum age range could be around 50 ka (Tomkins et al., 2018a), but could be even greater for areas with different lithologies or weathering rates (Matthews and Winkler, 2022).

Periglacial deposits are difficult to date (Rode and Kellerer-Pirklbauer, 2012) and are often associated with long periods of activity. Due to the homogenous lithology common in coarse periglacial deposits, the Schmidt hammer has been used for dating such deposits (Clark and Wilson, 2004; Wilson and Matthews, 2016; Wilson et al., 2017; Marr et al., 2022), including rock glaciers and protalus ramparts (Shakesby et al., 1987; Aoyama, 2005; Frauenfelder et al., 2005; Kellerer-Pirklbauer et al., 2008; Böhlert et al., 2011; Rode and Kellerer-Pirklbauer, 2012; Kłapyta, 2013; Matthews et al., 2013; Scapozza et al., 2014, 2021; Winkler and Lambiel, 2018; Nesje et al., 2021; de Marcos et al., 2022; Santos-González et al., 2022a).

In combination with other dating methods (i.e. cosmic ray exposure, CRE ages), it is possible to use control boulders of known ages to perform Schmidt hammer exposure–age (SHD or SHED) dating using a calibration curve (i.e. Shakesby et al., 2011; Matthews et al., 2015; Tomkins et al., 2016, 2018a, 2018b; Wilson and Matthews, 2016; Winkler and Lambiel, 2018; Marr et al., 2019; Wilson et al., 2019a, 2019b; Linge et al., 2020; Winkler et al., 2020; Matthews et al., 2023). This method has been recently extensively reviewed by Matthews and Winkler (2022).

Due to some advances in comparison with other techniques (including lower cost and rapid results), the Schmidt hammer is increasingly used for glacial and periglacial Quaternary research. However, important limitations to Schmidt hammer use remain, particularly that comparisons between samples are only possible when lithology is the same and weathering rates are similar (Kellerer-Pirklbauer et al., 2008; Matthews et al., 2013; Tomkins et al., 2016; Matthews and Winkler, 2022), which makes regional comparisons challenging.

The sampling strategy using Schmidt-hammer has been also a relevant topic. One of the main opportunities of this technique is that it is possible to test a larger number of

boulders than with other procedures (i.e. cosmogenic dating) without a cost increment. Due to that, several boulders are usually sampled. This seems to reduce uncertainties as many boulders are sampled, but is necessary to i) take consistent and comparable sampling in each study area and ii) minimise non-age-related influences on R-values (Matthews and Winkler, 2022). In that sense, it is important to choose only boulders that could reflect the deposition age, not the age of post-depositional processes. Because of that, some authors discarded potentially unrepresentative impacts (i.e. Kellerer-Pirklbauer et al., 2008; Kłapyta, 2013; Ffoulkes and Harrison, 2014; Tomkins et al., 2016). Also, the number of boulders without signs of being affected by post-depositional processes available could be a limitation in some cases. So, different strategies could be found, including a single impact in a large number of boulders (i.e. Matthews et al., 2014; 2015) or multiple impacts per boulder, usually when scarce boulders are available (i.e. Matthews et al., 2013; Nesje et al., 2021). Therefore, different study cases would require different case-related solutions (Matthews and Winkler, 2022).

During Last Glaciations, extensive ice sheets covered northern Europe, while in the Mediterranean area smaller glaciers covered mountainous areas (Hughes and Woodward, 2008). The chronology of the maximum glacial extension in the Mediterranean mountains remains in debate, but in some areas an earlier maximum than in the ice sheet occurred (García-Ruiz et al., 2003; Hughes, 2022). The rapid response of these glaciers to climate changes makes the study of glaciation specially relevant and is important to correlate marine and continental proxies to understand past circulation pattern.

The Cantabrian Mountains (NW Spain) range was glaciated during the Quaternary and shows well-developed glacial and periglacial landforms; however, chronological data

are scarce (Jiménez-Sánchez et al., 2022; Pellitero, 2022; Pérez-Alberti and Valcarcel, 2022; Ruiz-Fernández et al., 2022a, 2022b; Santos-González et al., 2022b; Serrano et al., 2022a, 2022b). Therefore, main glacial stages and the significance and formation of periglacial landforms, such as rock glaciers and blockfields, and their relation to the deglaciation process, are still poorly understood. Schmidt hammer can significantly help to better understand the geomorphological evolution of this area.

In this context, the objectives of this work are to:

i) Apply the Schmidt hammer to five different massifs in a geologically complex area to explore possible method limitations.

ii) Identify different glacial stages from the last glaciation.

iii) Analyse whether rock glaciers formed during the same cold stage (climate-related) or during different stages following the deglaciation process (paraglacial origin).

iv) Study the relative chronology of blockfields and other periglacial deposits, such as talus slopes.

2. Study area

The Cantabrian Mountains are in northwestern Spain, running parallel to the Cantabrian Sea, located only 25–80 km north of the main summits, and reaching 2000–2648 m a.s.l. (Fig. 1). This mountain range presents great geological diversity. In the west, Palaeozoic and Precambrian siliceous materials are dominant, including slate, quartzite, and sandstone. In the central and eastern parts, Paleozoic lutite, sandstone, and quartzarenite sandstone alternate with limestone and dolomite with complex geological structures, including overthrusts. Montes de León is located 50 km southwest of the

Cantabrian Mountains and shows similar characteristics to those of the western sector of the range.

Glacial (Santos-González et al., 2013, 2022b; Serrano et al., 2015, 2017, 2022a, 2022b; Jiménez-Sánchez et al., 2022; Pellitero, 2022; Pérez-Alberti and Valcarcel, 2022; Redondo-Vega et al., 2022; Ruiz-Fernández et al., 2016, 2022b) and periglacial (Redondo-Vega et al., 2010; Gómez-Villar et al., 2011; Pellitero et al., 2011; Pisabarro et al., 2017; González-Gutiérrez et al., 2019) landforms are widely distributed along the range, with small ice patches from the Little Ice Age (LIA) remaining in the highest areas (Serrano et al., 2018; Ruiz-Fernández et al., 2022a). Maximum glacial extension probably occurred prior to the Last Glacial Maximum (LGM), as indicated by chronological data in this range (Jalut et al., 2010; Moreno et al., 2010; Serrano et al., 2012, 2013; Frochoso et al., 2013; Ruiz-Fernández et al., 2016; Rodríguez-Rodríguez et al., 2017, 2018), when the Equilibrium Line Altitude (ELA) was between 1000–1800 m a.s.l., depending on the different massifs (Santos-González et al., 2013). Previous glaciations could also have occurred during Marine Isotope Stage (MIS) 5d and MIS 3, according to Rodríguez-Rodríguez et al. (2018).

FIGURE 1

Four massifs were selected on the southern slopes of the Cantabrian Mountains (Valdeprado, Arcos del Agua, San Isidro, and Peña Prieta), and one additional massif was selected in Montes de León (Vizcodillo) (Fig. 1).

Valdeprado comprises Cambrian and Lower Ordovician quartzite, sandstone, and slate (Cabos Series). This valley was part of the Sil Glacier Complex, the largest in the

Cantabrian Mountains (Santos-González et al., 2013, 2022b). Chronological data from the upper part of the basin indicate a glacial maximum prior to the LGM, probably before 35 ka (Jalut et al., 2010). The area analysed is located toward the headwaters of Busmor Valley, a tributary valley of Valdeprado, where two rock glaciers at different altitudes are present (Alonso, 1989; Alonso and Trombotto Liaudat, 2009; Redondo-Vega et al., 2010; Gómez-Villar et al., 2011; Santos-González, 2011; González-Gutiérrez et al., 2019). There are no chronological data, but another rock glacier and a debris avalanche located in the upper Sil basin (Muxivén peak) indicate that these deposits were formed during the deglaciation of the Bølling-Allerød interstadial (Santos-González et al., 2022a).

The Arcos del Agua massif is located in the southwesternmost part of the range. During the local LGM, a glacial tongue over 15 km long occupied the main Valle Gordo Valley (García de Celis and Martínez-Fernández, 2002; Santos-González et al., 2022b), but no clear moraines related to this stage have been identified. This study focuses on two glacial cirques on the northern slopes of Peña Cefera (2011 m a.s.l.) and Arcos del Agua (2063 m a.s.l.), as well as on the summit. The lithology is the same as that of Valdeprado, with the main periglacial deposits composed of quartzite from the Cabos Series. Some rock glaciers exist in this area at different altitudes (García de Celis, 1991; Redondo-Vega et al., 2010; Gómez-Villar et al., 2011a). In the cirque, small moraines surround closed depressions with ponds. Extensive blockfields exist at the summit and connect with large debris slopes (García de Celis, 2002).

San Isidro is in the central part of the Cantabrian Mountains. The area was occupied by a small icefield that generated a glacier over 16 km long (Rodríguez-Rodríguez et al., 2016, 2018) and left a notable imprint in the relief (Danis-Álvarez and Santos-González, 2017). The glacial maximum has been dated in the frontal area, where some large

erratics are present (Redondo-Vega et al., 2014), indicating the possibility of at least three glacial cycles (Rodríguez-Rodríguez et al., 2016, 2018). During glacial retreat, many rock glaciers were generated in glacial cirques (Rodríguez Pérez, 1995; Gómez-Villar et al., 2011; González-Gutiérrez et al., 2019; Rodríguez et al., 2022). One of these rock glaciers was dated by Rodríguez-Rodríguez et al. (2016), indicating an age of 15.2–16.3 ka for its stabilisation and 17.4–18.8 ka for deglaciation.

To the east, the Peña Prieta Massif (2539 m a.s.l.) is one of the highest in this range and contains abundant glacial and periglacial deposits (Pellitero, 2022). The local LGM occurred before 35 ka (Serrano et al., 2013), but the main lower moraines are related to the LGM (Pellitero et al., 2019). Other upper moraines are probably related to the Oldest Dryas (Pellitero et al., 2019). Small-rock glaciers are present in the highest cirques (Redondo-Vega et al., 2010; Gómez-Villar et al., 2011; Pellitero, 2014), but no chronological data exist. Periglacial landforms are widespread in the uppermost areas (Pisabarro et al., 2017) and the thermal regime of the uppermost rock glacier (in the Hoyo Empedrado upper valley) indicates that permafrost may be present in this area (Melón-Nava et al., 2022), so it could be an intact rock glacier rather than a relict glacier.

The Vizcodillo massif hosts most of the best-preserved glacial landforms in the Montes de León area (Stickel, 1929; Schmitz, 1969; Redondo-Vega et al., 2002b, 2022). This area has greater summer aridity than the massifs located in the Cantabrian Mountains. Three main moraine stages have been observed in this massif (Redondo-Vega et al., 2022), but no chronological data are available. Periglacial landforms appear in the upper part of the massif, including blockfields and ploughing boulders (Santos-González et al., 2016).

3. Methods

3.1. Schmidt-hammer procedures and sampling strategy

The electronic Proceq® Rock Schmidt hammer (Type N) was used, with an impact energy of 2.207 Nm. The instrument was new for this work and calibrated manually using a test anvil.

For a successful performance of the study, areas with preserved glacial and periglacial landforms related to different geomorphological stages and with lithological homogeneity were selected. For this purpose, the following criteria were used:

- Deglaciated areas with enough boulders available for sampling. For this reason, massifs composed of shale or slate could not be sampled due to the low number and small size of boulders. The calcareous massifs were also rejected because of their remarkable karstic features after deglaciation and rock micro-topography. Sandstone shows remarkable weathering features and poorly preserved landforms. Therefore, only quartzite, quartzarenite sandstone and granodiorite massifs were sampled.
- Areas where relict rock glaciers are located at different altitudes and past glacial environments: Valdeprado, Arcos del Agua, San Isidro, and Peña Prieta.
- Massifs with clear moraine ridges that are representative of different glacial stages: Vizcodillo and Peña Prieta.
- Areas with blockfields and adjacent glacial and periglacial deposits to compare relative ages: Vizcodillo and Arcos del Agua.

Several sample selection procedures were performed during sampling. Although fewer boulders than usual were sampled, the two golden rules defined by Matthews and Winkler (2022) were considered: *(1) consistent and comparable sampling and*

measurement must be followed for all sites within a particular study; and (2) the chosen strategy needs to be adapted to local conditions in order to minimise non-age-related influences on R-values and hence potential dating errors. These procedures were the same than in the work of Santos-González et al. (2022a).

- The same lithology was always chosen at each site, including mainly Ordovician quartzite (Valdeprado, Arcos del Agua, Muxivén), quartzarenite sandstone (San Isidro), and granodiorite (Peña Prieta).
- In moraines and rock glaciers, only stable boulders in ridges were selected (except in HP-09 where one furrow were sampled for comparison), in order to reduce the possible influence of the longer persistence of snow in furrows on R-values (Winkler and Lambiel, 2018). For erratics, only boulders over 1 m high were sampled. In blockfields and talus slopes, stable boulders in representative sections of the deposits were selected. In the rock outcrop and the polished bedrock, representative well-preserved sections of the sites were selected. The objective was to search sites that had not been affected by post-depositional processes.
- Only boulders over 50 cm in length (preferably 1 m) located in stable and prominent locations were selected, in order to avoid sampling boulders that may had been exhumed by erosion and to ensure that only subaerial erosion have occurred.
- Due to boulder limitations in some sites (mainly moraines and erratics), only six boulders were selected at each landform, except for sample HP-01, where only four boulders could be sampled, and sample VI-06, which was a polished threshold in the cirque where 40 impacts were performed. A total of 72–120 impacts per site (600–1440 per massif) were performed, varying between 20 impacts per boulder (Arcos del Agua, Valdeprado and Vizcodillo) and 12 impacts per boulder (San

Isidro and Peña Prieta). Outliers were not removed, but clearly anomalous readings (i.e. where non-visible cracks occurred) were. The sample selection procedures were similar to those for cosmogenic dating, seeking high-quality data instead of sampling multiple boulders with possible differences in geomorphological evolution, although losing an advantage of this method, such as the possibility of sampling a large number of boulders, especially in periglacial deposits.

- For each boulder, the impacts were restricted to flat and smooth surfaces, without visible cracks or weaknesses, and in lichen-free areas (Guglielmin et al., 2012).
- All data from each massif were collected on the same day, during sunny summer days and performed by the same person.

3.2. Sampling sites

A total of 4600 R-values were obtained from 48 sample sites in the five selected massifs (Table 1). Note that in each massif, not all the glacial / periglacial stages could be sampled, as some of them do not show suitable boulders for sampling.

TABLE 1

In Arcos del Agua, the following main glacial and periglacial landforms of the Peña Cefera and Arcos del Agua cirques (composed of quartzite) were selected:

- The Peña Cefera rock glacier, which is one of the longest in the Cantabrian Mountains (García de Celis, 1991; Redondo-Vega et al., 2010; Gómez-Villar et

al., 2011) and is one of the few rock glaciers that occurs outside a glacial cirque. Three sampling points were selected in the lower (AR-01) and central (AR-02 and AR-03) parts of the rock glacier at altitudes of 1600–1700 m a.s.l. The upper part was covered by talus slopes, where four measurements were taken in a debris cone (AR-04), a talus slope at the base of the cirque (AR-05), a recent (<10 years according previous field work) small debris fall composed of lichen-free boulders (AR-06), and the highest part of the talus slope (AR-07). All were located between 1750 and 1830 m a.s.l.

- Outside of the glacial cirques, on the southern side of the range are quartzite blockfields and talus slopes (García de Celis, 2002). Two samples were collected very close to the Peña Cefera peak (AR-08 and AR-09) at an altitude of approximately 2000 m a.s.l.
- In the Arcos del Agua cirque, Schmidt hammer measurements were performed in a small lobate rock glacier (AR-10), a small tongue-shaped rock glacier (AR-11), and a moraine (AR-12), all of which were located at an altitude of approximately 1900 m a.s.l.

In Valdeprado, two different rock glaciers composed of quartzite were sampled on the northern slope of the El Miro peak (1985 m a.s.l.), with the frontal parts located at 1720 m a.s.l. (in a glacial cirque) and 1545 m a.s.l. (over a glacial trough). The lower part shows some dense vegetation cover. Two samples were taken from two ridges (VP-01 and VP-02) and two other measurements were taken from two areas of the upper ridge (VP-04 and VP-05). The talus slope supplying the lower rock glacier (VP-03) was also sampled.

Nine sampling sites composed of quartzite were selected in Vizcodillo (Table 1). Two of these are related to the local LGM (Redondo-Vega et al., 2002b; 2022) (VI-01 and

VI-02). Two other samples were collected from the moraines that enclosed Lake Truchillas: one from the external moraine (VI-03) and the other from the internal moraine (VI-04). Two other samples were collected from a talus slope near the lake (VI-05) and on a polished bedrock in the upper part (VI-06). Three other samples were collected from the summit blockfields around the Vizcodillo peak (VI-07, VI-08, and VI-09).

In San Isidro, two rock glaciers were selected. The first was located SE of Lake Ausente in a glacial cirque, where a rock glacier composed of quartzarenite sandstone exhibit well-preserved furrow and ridge morphology. Its limits are well-defined and show a high front over the limestone outcrops. Three samples were collected from the lateral part (AU-01), a ridge in the inner part (AU-02), and the frontal part (AU-03). Chronological data exist for another rock glacier located immediately to the north (Rodríguez-Rodríguez et al., 2016), but no Schmidt hammer measurements were performed because of the high degree of sandstone weathering. The other rock glacier is located very close to the San Isidro ski resort and has been affected by a gravel pit that has dismantled its right lateral part. In this area, seven samples were collected: six on ridges along the rock glacier and one on the talus slope that supplied the rock glacier (SI-01 to SI-07).

In Peña Prieta, twelve sites composed of granodiorite were sampled. The lowest one (HP-01) include four erratic boulders in a difluence pass between Hoyo Empedrado and Naranco valleys. Another two samples were collected from the moraines that enclosed the Hoyo Empedrado pond (HP-02 and HP-03). In the cirque, two small rock glaciers, including their ridges (HP-05 and HP-08), frontal parts (HP-04) and furrows (HP-09), and their talus slopes supply areas (HP-06, HP-07, HP-10 and HP-11) were sampled. A rock outcrop of the cirque walls was also sampled (HP-12).

3.3. Geomorphological mapping and Statistics

The primary glacial and periglacial deposits of the five massifs were mapped based on fieldwork, orthophotos, and previous studies. Detailed geomorphological maps of the five areas were constructed using the ArcGIS Pro software. Unmanned aerial vehicle (UAV) was also used to obtain images and enhance geomorphological maps in all the study areas.

The Schmidt hammer rebound values were processed using Rstudio version 4.3.1. (R Core Team, 2022). For each location descriptive statistics, such as mean values, medians, standard deviation (SD) and 95% confidence intervals (CI) for the mean of the samples were calculated. Additionally, a boxplot representation was created using the ggplot library (Wickham, 2016) to display the R-values for each site, with labels indicating the location, lithology, and age dating information for some samples.

A Kruskal-Wallis test was performed, revealing a significant difference among the lithological groups (quartzite, quartzarenite sandstone, and granodiorite) with a p-value of 6.348e-08. Subsequently, pairwise comparisons were conducted using the Wilcoxon rank-sum exact test with Bonferroni correction. These pairwise comparisons identified statistically significant differences between all lithological groups, with the most significant differences observed between quartzites and granodiorites. Consequently, a density plot was created using the ggdensity library (Otto and Kahle, 2023) to visualize differences between site means and standard deviations based on lithology.

4. Results

Over 4600 R-values obtained for the 48 sample sites of the five massifs analysed are summarised in Table 2 and shown in Fig. 2. Another 780 R-values obtained in a previous study in the Muxivén area (Santos-González et al., 2022a) are included for comparison in Fig. 2.

TABLE 2

FIGURE 2

The data show small differences in the mean and median R-values. The SD range between 2.0 and 12.8, with higher values in Peña Prieta and San Isidro, and lower values for quartzites. The CI also increased in the former areas compared with the latter.

Detailed data for each massif, including geomorphological maps and site overviews, are presented in the following subsections.

4.1. Arcos del Agua

The mean R-value data show clear differences between the sampled landforms and SD values from 2.4 to 5.2 (Fig. 3, Fig. 4).

- Lower values in the tongue-shaped rock glacier, ranging between 70.7 in the frontal part, and 72.0 and 71.7 in the central part.
- The moraine that encloses the Arcos del Agua pond gives R-values of 73.1, slightly lower than the values for the rock glacier located in the cirque (74.0), the

debris cone that cover the tongue-shaped rock glacier (74.4), and the lobate rock glacier (75.0).

- The two sampled blockfields in the summit area show R-values from 74.9 to 76.8.
- Talus slopes in the Peña Cefera cirque present R-values that increase from 76.2 at the cirque floor to 77.4 at the highest part of the cirque. A recent (<10 years) rockfall deposit near the cirque bottom has R-values of 78.0.

FIGURE 3

FIGURE 4

4.2. Valdeprado

Two rock glaciers were sampled in the upper part of Busmor Valley (Fig. 5). The results show significant differences between the lower and upper rock glaciers. In the lower rock glacier, the values ranged between 65.8 and 69.2, while in the upper rock glacier, values ranged between 74.4 and 75.5. A talus slope showing recent activity was also sampled and presented an R-value of 76.6. SD ranged from 2.5 to 6.8, with higher values in the lower rock glacier.

The vegetation cover of the two rock glaciers is also noticeable. The lower part clearly shows denser vegetation cover than the upper part, where vegetation covers only the front part of the rock glacier (Fig. 6).

FIGURE 5

FIGURE 6

4.3. Vizcodillo

In the Vizcodillo massif, different glacial and periglacial landforms were sampled, revealing some differences between the sampled sites (Fig. 7, Fig. 8):

- The lower moraines of the Millín and Del Lago valleys showed similar values of 73.9 and 74.1, respectively.
- The moraines that enclosed Lake Truchillas exhibited different values. The external moraine had mean R-values of 75.2 and the internal had R-values of 76.8.
- A talus slope in the lake margin provided a slightly higher value (77.3).
- A polished threshold at the top of the cirque also showed a value similar to the talus slope (77.5).
- The samples in the blockfields located near Vizcodillo peak ranged between 78.8 and 79.6.

SD values were low, ranging between 2.0 and 4.3.

FIGURE 7

FIGURE 8

4.4. San Isidro

The sampled sites and mean R-values in the San Isidro area are shown in Fig. 9 and Fig. 10. The rock glacier located near the San Isidro ski resort presented very similar mean values throughout its surface ranging from 73.0 to 74.3. The talus slope sampled immediately south of the rock glacier exhibited similar values.

In contrast, greater differences were observed in the Ausente rock glacier, which is composed of more intensely weathered quartzarenite sandstone. In this case, the two ridges at the frontal part of the rock glacier gave mean R-values of 67.6 and 69.9. The lateral ridge of the rock glacier showed a lower value (63.3). In any case, mean SD was high (8.0) in the Ausente rock glacier, and greater than for the Cebolledo rock glacier (4.3).

FIGURE 9

FIGURE 10

4.5. Peña Prieta

The R-values in Peña Prieta showed greater differences than in other massifs, and also higher SD values (mean: 8.0) (Fig. 11 and Fig. 12):

- Four erratic boulders located in a difluence pass from the Hoyo Empedrado valley indicated an R-value of 37.0.

- The moraines that enclosed the Hoyo Empedrado Pond gave mean R-values of 52.9 and 57.3.
- Two small lobate rock glaciers in the upper part of the cirque showed R-values of 61.0 for the front of the lower rock glacier, 65.6 and 67.2 in the frontal ridge of the lower and upper rock glacier, respectively, and 69.1 in the furrow of the upper rock glacier.
- The talus slopes that supplied debris to the rock glaciers showed R-values ranging from 67.1 and 67.9 for the lower slopes, and 69.2 to 70.4 in the upper slopes.

In the rock wall located in the upper part of the cirque, an R-value of 67.8 was obtained.

FIGURE 11

FIGURE 12

5. Interpretation and Discussion

5.1. Geomorphological evolution and probable chronology

The R-value data showed significant differences related to lithology and deposit age. Although the SD values generate uncertainty and more chronological data are needed, the R-values show a geomorphological evolutionary sequence in each massif, which allows several stages to be established. These phases are relatively similar between massifs, so it is possible to correlate them with each other. Moreover, they can be

related to the known chronological evolution of some massifs in the Cantabrian Mountains and elsewhere in the Iberian Peninsula, establishing a tentative chronology for all the sites sampled (Fig. 13).

FIGURE 13

Stage 1) The most external deposits analyzed are the lower moraine of Vizcodillo and some erratics in Peña Prieta. The R-value data differed notably for the quartzite boulders from Vizcodillo (73.8 and 74.1) than for the granodiorite boulders from Peña Prieta (37.0); however, both cases showed the lowest values in their respective study areas (Fig. 13). In Peña Prieta, two erratic boulders in the same location were sampled by Pellitero et al. (2019) using ^{10}Be exposure dating, obtaining 15.7 and 20.0 ka, so it was not clear if they were related to the LGM or to the Oldest Dryas. In other massifs, such as Arcos del Agua and Valdeprado, moraines of the local LGM are very scarce or non-existent because of the unfavourable topographic conditions for their deposition and preservation (Santos-González et al., 2018). Although previous glacial stages probably occurred in the Cantabrian Mountains (Rodríguez-Rodríguez et al., 2016, 2018), the local LGM probably occurred prior to the LGM at approximately 35 ka (Jalut et al., 2010; Moreno et al., 2010; Frochoso et al., 2013; Serrano et al., 2012, 2013; Rodríguez-Rodríguez et al., 2017, 2018). In many massifs, moraines probably reached similar positions during the LGM; however, data on these periods remains scarce (Pellitero, 2022; Rodríguez-Rodríguez et al., 2022; Santos-González et al., 2022b). Given the R-values and geomorphological context, the external deposits sampled in this

work were probably deposited during the LGM, but could also be related to previous advances.

Stage 2) After the LGM, glaciers retreated to the highest areas. During this recession, the lower rock glaciers of Valdeprado and Arcos del Agua likely formed. The data in both areas clearly indicate lower values for these rock glaciers than for the upper ones, and also lower values for the moraine in the Arcos del Agua cirque (Fig. 13). This stage should occur after the deglaciation of the main valleys, which usually occurred after the LGM (Serrano et al., 2015, 2022a, 2022b; Jiménez-Sánchez et al., 2022; Pellitero, 2022; Pérez-Alberti and Valcarcel, 2022; Redondo-Vega et al., 2022; Ruiz-Fernández et al., 2022b; Santos-González et al., 2022b), and before the moraines in the cirques, because the R-values of these rock glaciers show intermediate values. So, these rock glaciers probably occur just after the LGM, only where topographic conditions were favourable for the genesis of rock glaciers.

Stage 3) The R-value data in the moraines in the Arcos del Agua and Vizcodillo cirques (AR-12, VI-03, and VI-04) and those that enclosed Hoyo Empedrado Pond (HP-02 and HP-03, Peña Prieta massif), show an intermediate stage with glaciers restricted to cirques (Arcos del Agua and Vizcodillo) or generating small tongues in the highest areas (Peña Prieta). These moraines likely formed during the Oldest Dryas, when glaciers were usually restricted to cirques in the Cantabrian Mountains (Oliva et al., 2023a). In San Isidro, the glaciers retreated strongly at 17.7 ka (Rodríguez-Rodríguez et al., 2016, 2018), but the extension during the Oldest Dryas has not been reconstructed and no moraines of this area were sampled in this work.

Stage 4) R-values in the upper rock glaciers of Arcos del Agua and Valdeprado indicate that they stabilized slightly later than the formation of earlier moraines. The large contributions of debris necessary to form the rock glaciers are indicative of extensive

deglaciation of the cirque walls, which favoured paraglacial dynamics. This process occurred during the Bølling–Allerød warming when glaciers disappeared in many massifs or became restricted to the uppermost areas (Oliva et al., 2023a). During this retreat, the conditions were favourable for permafrost occurrence and for intense paraglacial dynamics, as the cirque walls supplied high quantities of debris over glacier remnants. In the Muxivén area, a rock avalanche formed and contributed to formation of rock glaciers and a debris avalanche, which stabilized at 14–13.5 ka (Santos-González et al., 2022a). Similar processes have been shown for rock glaciers in San Isidro (Rodríguez-Rodríguez et al., 2016) and Redes (Rodríguez-Rodríguez et al., 2017), where the upper rock glaciers stabilised slightly later than the lower ones. So, during this period, the rock glaciers of San Isidro (AU, SI) and the upper rock glaciers of Arcos del Agua (AR-10, AR-11) and Valdeprado (VP-04, VP-05) likely formed and stabilised, as probably occurred for most of the rock glaciers in the Cantabrian Mountains. The lower talus slopes probably also stabilized during this period.

Stage 5) In Vizcodillo, the internal moraine of Lake Truchillas had a higher R-value than the external one, which indicates that they could be formed in different glacial stages, although R-value differences are small and in the range of SD. This stage, only observed in this massif, could have formed during the Younger Dryas, a period in which small glaciers could have occurred, but no chronological data exist for NW Spain (Oliva et al., 2023b). In any case, the data is insufficient to have a clear view, and it could also be related to other periods, as the Bølling–Allerød.

Stage 6) In cirques, talus slopes show higher R-values than moraines and rock glaciers, indicating that they were subsequently stabilized. In some favourable areas, some dynamics still persist (AR-06). These talus slopes are common in all areas and have been sampled in Arcos del Agua, Valdeprado, Vizcodillo and San Isidro. They are also

common in most of the mountain range and were frequently formed during deglaciation (i.e. Ruiz-Fernández et al., 2016), although there are few detailed studies on them (i.e. Peña-Pérez, 2021). The high R-values in the upper part of the Vizcodillo cirque (VI-06) may also indicate glacial activity close to the Holocene.

The R-values of the blockfields in Arcos del Agua and Vizcodillo indicate that many of them were also active after cirque deglaciation. Some of them show very high R-values and probably stabilized during the LIA, but others could only be active during other previous cold periods of the Holocene.

In Peña Prieta, the higher altitude compared to the rest of the massifs could allow the genesis of periglacial landforms during the Holocene. The R-value indicates two different stages of formation of small lobate rock glaciers in the cirque. Both could have stabilized during the Holocene and the upper one (HP-08) probably during the LIA. During the LIA small glacier was observed in a nearby cirque (Prado, 1852) and some small glaciers developed in the highest areas of Picos de Europa (Serrano et al., 2018; Ruiz-Fernández et al., 2022a). Although no recent movements have been observed in this rock glacier, the thermal regime indicates that permafrost is possible (Melón-Nava et al., 2022), so it could be an intact rather than a relict rock glacier. The R-values also show more recent dynamics for the upper talus slopes of the slope than for the lower ones. Most of them were probably active at the beginning of the Holocene and progressively ceased activity, with the highest areas the last to stabilise.

5.2. Rock glaciers generation in relation with deglaciation

Relict rock glaciers are widespread in the Cantabrian Mountains (Redondo-Vega et al., 2010; Gómez-Villar et al., 2011; Pellitero et al., 2011; González-Gutiérrez et al., 2019),

but chronological data only exist for rock glaciers in the areas of San Isidro (Rodríguez-Rodríguez et al., 2016), Redes (Rodríguez-Rodríguez et al., 2017), and Muxivén (Santos-González et al., 2022a). In all three cases, the rock glaciers are related to deglaciation, probably during the Bølling-Allerød interstadial, with the higher rock glaciers stabilising slightly later (~13 ka) than the lower rock glaciers (14-15.7 ka). The relationship between relatively warm periods and the generation of rock glaciers has been observed in some areas, such as in the Alps (Böhlert et al., 2011; Scapozza et al., 2014, 2021). Therefore, many studies suggest a paraglacial origin for rock glaciers, rather than formed during a cold stage (Linge et al., 2020; Palacios et al., 2021; Oliva et al., 2022).

Rock glaciers of the Cantabrian Mountains only occur in deglaciated areas affected by an alpine style of glaciation that, with favourable lithological conditions, generates sufficient debris supply, indicating a paraglacial dependence of rock glaciers (Santos-González et al., 2018). The same geomorphological environment has been observed in other mountainous areas (Onaca et al., 2017). In that sense, in addition to permafrost occurrence, the availability of steep rock walls for debris production has been shown as a main factor controlling the distribution of rock glaciers (i.e. Onaca et al., 2017), and in the Cantabrian Mountains, this rarely occurs outside of glacial cirques and some over-deepened glacial valleys, and preferable just after glacial retreat due to paraglacial dynamics (Ballantyne, 2002). Because of that, the majority of the rock glaciers in the Cantabrian Mountains occur in cirques, whereas some occur in upper glacial valleys (Gómez-Villar et al., 2011).

In this study, two rock glaciers located in glacial valleys were sampled and compared to nearby rock glaciers located at higher altitudes, in the cirques (Valdeprado and Arcos del Agua). In both cases, the rock glaciers at higher altitudes showed higher R-values

than those at lower altitudes. These data indicate that, although many of the rock glaciers probably occurred during deglaciation in the Bølling-Allerød interstadial or at the end of the Oldest Dryas / Heinrich Stadial 1, some rock glaciers stabilised at an earlier stage, probably just after or during the LGM. Furthermore, in the highest areas, such as Peña Prieta, rock glaciers were formed during the Holocene.

The R-value data are indicative of rock glacier stabilisation, which could occur thousands of years after initial rock glacier generation, raising doubts about the applicability of the method (Matthews et al., 2013). But previous Schmidt hammer studies have shown consistent data for rock glaciers (i.e. Winkler and Lambiel, 2018), instead of, in some cases, SHD results indicate long periods of rock glacier formation (Rode and Kellerer-Pirklbauer, 2012), or notable differences between the stabilisation of the rooting zone and the front (Scapozza et al., 2014).

In the Cantabrian Mountains, rock glaciers are usually small and consistent data were obtained where multiple samples were taken from the same rock glacier (San Isidro) indicating that stabilisation occurs at the same or similar time in many cases. However, in other areas, R-value differences could indicate that the internal parts of the rock glaciers stabilised later than the frontal or lower parts (Arcos del Agua). In many Iberian mountain areas, rapid stabilisation of rock glaciers shortly after their formation has been observed (Oliva et al., 2023a). This is the case for the Muxivén rock glaciers, where rock avalanches and paraglacial processes in the cirque contributed to rock glacier formation (Santos-González et al., 2022a).

Age differences in rock glaciers have been previously noted by other authors based on geomorphological sequences, such as in the Ancares range (Valcárcel-Díaz and Pérez-Alberti, 2002), Valdeprado (Alonso and Trombotto Liaudat (2009) and Arcos del Agua (García de Celis, 2002). Pioneering works in the Pyrenees suggested that rock glaciers

formed during the same stage after deglaciation, whereas more recent studies have shown different generation mechanisms for rock glaciers (Serrano, 2014; Oliva et al., 2016), and a clear relationship with deglaciation processes driven by paraglacial rather than climatic dynamics (i.e. Palacios et al., 2015). Because of this, although many Iberian rock glaciers have ages of 15–13.5 ka (Rodríguez-Rodríguez et al., 2016; Palacios et al., 2017; Andrés et al., 2018; García-Ruiz et al., 2020; Santos-González et al., 2022a; Fernandes et al., 2023), shortly after a glacial advance at ~16 ka and following an abrupt climate change (Cacho, 2022), others were formed during different periods (Oliva et al., 2016) or still remain active (Chueca and Julián, 2005; Serrano et al., 2010; Martínez-Fernández et al., 2019).

The results of the present study show that, although many rock glaciers in the Cantabrian Mountains may have occurred during the Bølling-Allerød interstadial or at the end of the Oldest Dryas, others (such as the lower rock glaciers of Valdeprado and Arcos del Agua) developed before outside of glacial cirques . These were probably coeval with glaciers that occupied the cirques during the main deglaciation, just after the LGM. This process occurred only at locations with a sufficient debris supply from the lateral valley walls. Inside cirques, small differences also occurred depending on location (Redondo-Vega et al., 2002a), as the Arcos del Agua data suggest; however, further research is required. Furthermore, in the highest cirques such as Peña Prieta, some rock glaciers were related to the deglaciation of the highest cirques during the Holocene.

5.3. Age and dynamics of blockfields

Blockfields were sampled in Vizcodillo and Arcos del Agua. In both areas, the blockfields are located immediately above glacial cirques, at higher altitudes, and were likely not affected by Quaternary glaciers. Several blockfields exist in the Cantabrian Mountains and NW Spain, and are usually connected with more extensive block slopes (Pérez-Alberti and Rodríguez-Guitián, 1993; García de Celis, 2002; Valcárcel-Díaz and Pérez-Alberti, 2002; Pellitero, 2009; Santos González, 2011; Oliva et al., 2016).

Blockfields ages in the Cantabrian Mountains remain controversial. Pellitero (2009) suggest that blockfields only occurred outside the glaciated area; therefore, they had to have formed prior to or simultaneous with the LGM, as some blockfields were cut by glacial erosion. In contrast, Valcárcel-Díaz and Pérez-Alberti (2002) reported that blockfields are located in glaciated areas in the westernmost area of the Cantabrian Mountains; therefore, they likely formed during or after the last glaciation, perhaps when small glaciers occurred in cirques, but they did not rule out the possibility that blockfields could also have been preserved from earlier stages under cold-based glaciers in some locations. Viana-Soto and Pérez-Alberti (2019) associated blockfield deposits with the LGM, when glaciers receded after the local LGM and cold conditions prevailed. In Arcos del Agua, García de Celis (2002) hypothesised that blockfields stabilized at similar stages to rock glaciers because of similar vegetation cover and boulders appearance. In Central Spain, an exposure age of ca. 83 ka was obtained for one boulder of a blockfield (Palacios et al., 2012).

In Arcos del Agua and Vizcodillo, the R-values indicated that stabilisation of these landforms occurred after the (almost) complete deglaciation of the glacial cirques. Owing to the scarcity of absolute chronological data, it is not possible to assign a definitive age for landform formation; however, blockfields stabilisation was probably related to cold stages during the Holocene. In any case, the origin of the blockfields

could be related to previous glacial stages, and they could be active again in later periods.

Some studies in northern Europe have indicated that, rather than being a Neogene weathering remnant, blockfields have a Quaternary origin (Goodfellow et al., 2014; Hopkinson and Ballantyne, 2014), whereas others have shown the complex and long-term activity of these landforms in very different geographical areas, such as Norway (Marr et al., 2018), the Sudetes (Engel & Braucher, 2020), Australia (Barrows et al., 2004) or NE United States (Denn et al., 2018), among others, indicating the transformation of this landforms during several cold periods. In a recent study, Marr et al. (2022) inferred that blockfields could have formed prior to the LGM and later reactivated during a cold event. This complex evolution and preservation during the cold-based ice stage was also reported by Wilson and Matthews (2016), who observed stabilisation of the blockfield during the early Holocene. The preservation of blockfields under cold-based ice (and blockfield evolution throughout much or all of the Quaternary) has been reported in previous studies in northern Europe (i.e. Goehring et al., 2008; Fabel et al., 2012; Ballantyne and Stone, 2015).

More data are required to clarify the formation of blockfields and activity stages in the Cantabrian Mountains. The Schmidt hammer data suggest that blockfields were still active after deglaciation, but their formation age remains an open question. Furthermore, only some blockfields were sampled and probably more boulders should be sampled in each blockfield, as these landforms could have a longer and more complex history than moraines or rock glaciers; therefore, more research is required to show whether the different blockfields became inactive at similar stages.

5.4. Influence of lithology in R-value data and implications for Schmidt hammer chronology

The Schmidt hammer has been shown as an effective tool for geomorphological reconstruction in several studies, especially during the last decade (i.e. Shakesby et al., 2011; Matthews et al., 2015; Tomkins et al., 2016, 2018a, 2018b; Wilson and Matthews, 2016; Winkler and Lambiel, 2018; Marr et al., 2019; Wilson et al., 2019a, 2019b; Linge et al., 2020; Winkler et al., 2020). In all five study areas, the R-value data correlated well with the geomorphological sequence, indicating that R-values are indicative of greater weathering. Many factors introduce uncertainty in the application of the Schmidt hammer, such as instrument wear (Shakesby et al., 2006), operator variance (Viles et al., 2011), and possible reworking of deposits (Evans et al., 1999), among others (Matthews and Winkler, 2022). Furthermore, gradual degradation arising from weathering can restrict Schmidt hammer dating to a specific period (Černá and Engel, 2011). However, dating is dependent on the lithology and weathering rates, which could also vary between glacial and interglacial periods (Matthews and Winkler, 2022).

Lithology plays an important role in the R-value data because the Schmidt hammer measurements reflect the compressive strength of the rock. Therefore, it is not possible to compare R-value data from different lithologies or with notable differences in climate (that influence weathering rates) (Kellerer-Pirklbauer et al., 2008; Tomkins et al., 2016; Matthews and Winkler, 2022). In complex geological areas such as the Cantabrian Mountains, where lithological changes are very frequent, this limits the application of the method because it is necessary to create multiple calibration curves depending on rock characteristics and weathering rates. Even small differences in the same rock type could influence the R-values, as has been shown in this work between the Ordovician quartzite of the Barrios Fm. (Muxivén) and Cambrian-Ordovician quartzite of the Cabos

Series (Valdeprado and Arcos del Agua). Therefore, a major task when comparing R-values is to avoid lithological differences during sampling in the same area (Matthews et al., 2013; Matthews and Winkler, 2022).

In this study, quartzite exhibited the highest R-values and lowest weathering rates (Fig. 14a). Quartz shows much slower weathering rates than other minerals and therefore exhibits limited R-value variation (Owen et al., 2007; Tomkins et al., 2016). High R-values have also been observed for quartzite in previous studies (Tomkins et al., 2016). For example, the Vizcodillo moraines, which should be related to the LGM, showed R-values of 73.8 and 74.1, slightly lower than those for the moraines likely related to the Oldest Dryas (75.2). Slightly higher decline rates have been observed in Arcos del Agua, where the lower rock glaciers, probably related to the LGM, gave R-values of 70.7, 71.7, and 72.0, whereas the recent talus slope gave an R-value of 78.0.

FIGURE 14

In contrast, the granodiorite showed larger differences between sampled sites (Fig. 14a). Erratic boulders, probably from the LGM (Pellitero et al., 2019) in a difluence pass, showed R-values of 37.0, while the moraine that likely formed during the Oldest Dryas gave R-values of 52.9 and 57.3. The rock glaciers and talus slope formed in one of the highest cirques in the range, gave R-values between 61.0 to 70.4. Granodiorite showed a significantly higher SD than quartzite (Fig. 14b). This could be related to the variation in mineral composition, which influences the R-values, as observed in Schmidt hammer testing of gneiss (Tomkins et al., 2016). Therefore, careful sampling selection is necessary. However, if there are clear age differences between the sampled sites, such

as in Peña Prieta, good results can be obtained, as has also been demonstrated for granite (i.e. Tomkins et al., 2018a) and gneiss (Rode and Kellerer-Pirklbauer, 2012; de Marcos et al., 2022).

Quartzarenite sandstones show an intermediate evolution and have been sampled in San Isidro, but are also present in other mountains in the range. In this massif, the Ausente rock glacier dated by Rodríguez-Rodríguez et al. (2016) could not be sampled because of the high weathering rates of sandstone boulders. Sandstone exhibited significant surface weathering (Fig. 8C), which appears to be nonlinear, as indicated by Tomkins et al. (2016). For this reason, sandstones appear to not be suitable, or present many difficulties, for the application of the Schmidt hammer.

As the age–calibration curve depends on a rock's resistance to subaerial weathering, which depends on the rock type and weathering rates in the study area (Matthews and Winkler, 2022), data from the present work imply that:

- Due to the slow weathering rates, for quartz-rich rocks, such as quartzite, it is more difficult to establish a Schmidt hammer calibration curve, and small age differences cannot be detected. However, high resistance to weathering could offer the opportunity to date a wider range of time, perhaps even previous glaciations. In contrast, granodiorite offers a better Schmidt hammer calibration curve and allows smaller age differences to be differentiated; however, higher rock weathering rates could limit the possibility of dating ancient deposits.
- Small differences in lithological composition affected the R-value data. For example, present-day deposits in Muxivén (Barrios quartzite) gave an R-value of 79.9, compared with 78.0 in Arcos del Agua (Cabos Series quartzite). The weathering rates are also slightly different. To compare data and obtain good

results, it is critical to carefully select sites to reduce the effects of lithological variability (Matthews and Winkler, 2022).

To present an adequate calibration curve for the Cantabrian Mountains, such as that obtained for the Pyrenees (Tomkins et al., 2018a), more chronological control points are necessary because minor errors significantly alter the calculated exposure age (Tomkins et al., 2016). For this purpose, future studies must consider possible differences in weathering rate changes between the LGM and the present (Linge et al., 2020; Scapozza et al., 2021; Matthews and Winkler, 2022).

Careful selection of boulders and sampling sizes are other major tasks. For this work, a comparison has been made between glacial deposits (many of them with very few boulders available) and periglacial deposits (which include many more boulders). Although most work argues that every suitable boulder available for sampling should be sampled to ensure that a representative sample is achieved (Matthews and Winkler, 2022) is also relevant to ensure that only boulders not affected by postdepositional processes and without signs of exhumation are sampled, in order to obtain the depositional age. In this work, the low number of boulders sampled may have affected data representativeness in some cases, especially in periglacial deposits, which may have a more complex depositional history. However, the careful selection of boulders (and the surfaces sampled in each boulder) has probably also contributed to not sampling boulders (and surfaces) affected by post-depositional processes.

6. Conclusions

The main conclusions of the work are summarized as:

- The application of the Schmidt hammer to five different massifs in NW Spain showed R-values indicative of a geomorphological evolutionary sequence of glacial and periglacial deposits formed during different stages. In any case, the small number of boulders sampled could reduce the significance of the data in some cases, especially for blockfields.
- In two areas (Valdeprado and Arcos del Agua), there was a clear relative age difference between the lower and upper rock glaciers. The lower ones stabilized immediately after or during the LGM. The upper rock glaciers, and others studied in San Isidro (as those previously dated in the range) are probably related to deglaciation processes during the Bølling–Allerød interstadial. The highest rock glaciers in the range (Peña Prieta) likely formed during the Holocene. These data support the idea of paraglacial control rather than climate dependence in the generation of rock glaciers.
- Talus slopes formed after deglaciation, and the R-value data indicate that they progressively become inactive from lower to higher altitudes.
- The sampled blockfields showed strikingly young ages, indicating that they probably stabilised during the Holocene. More research is required to chronologically locate blockfields during their geomorphological evolution.
- Relevant differences were found between the R-value data and weathering rates of quartzite, quartzarenite sandstones, and granodiorite. Quartzites show a very low R-value decrease with time, allowing dating of older deposits but unsuccessfully distinguishing deposits with little age difference. In contrast, granodiorite shows a greater decrease in the R-value with time, which could allow the differentiation of deposits with little age difference but not ancient deposits. Quartzarenite sandstones show intermediate values but cannot be

tested properly because of the poor preservation of low-altitude deposits. Other lithologies could not be sampled due to the scarcity of boulders (slates, shales) or due to intense weathering (sandstones, limestones).

- More chronological data are required to construct a proper calibration curve for absolute Schmidt hammer dating in the Cantabrian Mountains, which must be different for each lithological zone.

Acknowledgements: This research was supported by the project LE080G19 (Paleoenvironmental significance and relationship with the global change of the Cantabrian Mountains rock glaciers: relative age dating and analysis of the internal structure using electrical tomography), founded by the Junta de Castilla y León and the project 2022/00232/001 "Environmental dynamics, characteristics and potential use of pit lakes in northwestern Spain" founded by the Universidad de León. Adrián Melón-Nava was supported by the FPU program from the Spanish Ministerio de Universidades (FPU20/01220). We sincerely appreciate the comments and suggestions of the reviewers that have improved the first version of the manuscript.

References

Alonso, V., 1989. Glaciares rocosos fósiles en el área de Degaña-Leitariegos (Occidente de Asturias, Cordillera Cantábrica). Cuaternario y Geomorfol. 3 (1-4), 9–15. http://tierra.rediris.es/CuaternarioyGeomorfologia/images/vol3/cuaternario3%281-4%29_002-.pdf

Alonso, V., Trombotto Liaudat, D.T., 2009. Periglacial geomorphology of El Miro area, Cantabrian Mountains, NW Spain. Zeitschrift fur Geomorphol. 53 (3), 335–357.

https://doi.org/10.1127/0372-8854/2009/0053-0335

Anderson, E., Harrison, S., Passmore, D.G., Mighall, T.M., 1998. Geomorphic evidence of younger dryas glaciation in the Macgillycuddy's reeks, South West Ireland. J. Quat. Sci. 13 (6), 75–90.

Andrés, N., Gómez-Ortiz, A., Fernández-Fernández, J.M., Tanarro, L.M., Salvador-Franch, F., Oliva, M., Palacios, D., 2018. Timing of deglaciation and rock glacier origin in the southeastern Pyrenees: a review and new data. Boreas 47 (4), 973-1244. https://doi.org/10.1111/bor.12324

Aoyama, M., 2005. Rock glaciers in the northern Japanese Alps: palaeoenvironmental implications since the Late Glacial. J. Quat. Sci. 20 (5), 471–484. https://doi.org/10.1002/jqs.935

Ballantyne, C.K., 1997. Periglacial trimlines in the Scottish Highlands. Quat. Int. 38–39, 119–136. https://doi.org/10.1016/S1040-6182(96)00016-X

Ballantyne, C.K., 1998. Paraglacial geomorphology. Quat. Sci. Rev. 21 (18-19), 1935-2017. https://doi.org/10.1016/S0277-3791(02)00005-7

Ballantyne, C.K., Stone, J.O., 2015. Trimlines, blockfields and the vertical extent of the last ice sheet in southern Ireland. Boreas 44 (2), 277–287. https://doi.org/10.1111/bor.12109

Barrows, T., Stone, J.O., Fifield, L.K., 2004. Exposure ages for Pleistocene periglacial deposits in Australia. Quat. Sci. Rev. 23, 697–708. https://doi.org/10.1016/j.quascirev.2003.10.011

Böhlert, R., Compeer, M., Egli, M., Brandová, D., Maisch, M., Kubik, P., Haeberli, W., 2011. A Combination of Relative-Numerical Dating Methods Indicates Two High Alpine Rock Glacier Activity Phases After the Glacier Advance of the Younger Dryas. Open Geogr. J. 4, 115–130. https://doi.org/10.2174/1874923201003010115

Cacho, I., 2022. Quaternary ice ages in the Iberian Peninsula, in: Oliva, M., Palacios, D., Fernández-Fernández, J.M. (Eds.), Iberia, Land of Glaciers. Elsevier, pp. 13–35. https://doi.org/10.1016/B978-0-12-821941-6.00002-5

Černá, B., Engel, Z., 2011. Surface and sub-surface Schmidt hammer rebound value variation for a granite outcrop. Earth Surf. Process. Landf. 36 (2), 170–179. https://doi.org/10.1002/esp.2029

Chueca, J., Julián, A. 2005. Movement of Besiberris rock glacier, Central Pyrenees, Spain: data from a 10-year geodetic survey. Arct. Antarct. Alp. Res. 37, 163–170. https://doi.org/10.1657/1523-0430(2005)037[0163:MOBRGC]2.0.CO;2

Clark, R., Wilson, P., 2004. A rock avalanche deposit in Burtness Comb, Lake District, northwest England. Geol. J. 39 (3-4), 419–430. https://doi.org/10.1002/gj.965

Danis-Álvarez, P.J., Santos-González, J., 2017. Glacial influence on drainage network: Respina and Rebueno valleys (upper Porma basin, Cantabrian mountains, Northwest Spain). Cuad. Investig. Geogr. 43 (1), 269-291. https://doi.org/10.18172/cig.3037

de Marcos, J., Úbeda, J., Andrés, N., Palacios, D., 2022. A combination of cosmogenic and Schmidt hammer exposure dating in the study of the deglaciation timing of Sierra de Guadarrama National Park (Spain). Geogr. Ann. Ser. A, Phys. Geogr. 104 (2), 70–89. https://doi.org/10.1080/04353676.2022.2054146

Denn, A.R., Bierman, P.R., Zimmerman, S.R.H., Caffee, M.W., Corbett, L.B., Kirby, E., 2018. Cosmogenic nuclides indicate that boulder fields are dynamic, ancient, multigenerational features. GSA Today 4–10. https://doi.org/10.1130/GSATG340A.1

Engel, Z., 2007. Measurement and age assignment of intact rock strength in the Krkonose Mountains, Czech Republic. Z Geomorphol Suppl. 51 (1), 69–80.

https://doi.org/10.1127/0372-8854/2007/0051S-0069

Engel, Z., Braucher, R., Aumaître, G., Bourlès, D., Keddadouche, K., 2020. Origin and 10Be surface exposure dating of a coarse debris accumulation in the Hrubý Jeseník Mountains, Central Europe. Geomorphology 365, 107292. https://doi.org/10.1016/j.geomorph.2020.107292

Evans, D.J.A., Archer, S., Wilson, D.J.H., 1999. A comparison of the lichenometric and Schmidt hammer dating techniques based on data from the proglacial areas of some Icelandic glaciers. Quat. Sci. Rev. 18, 13–41. https://doi.org/10.1016/S0277-3791(98)00098-5

Fabel, D., Ballantyne, C.K., Xu, S., 2012. Trimlines, blockfields, mountain-top erratics and the vertical dimensions of the last British–Irish Ice Sheet in NW Scotland. Quat. Sci. Rev. 55, 91–102. https://doi.org/10.1016/j.quascirev.2012.09.002

Fernandes, M., Oliva, M., Fernández-Fernández, J.M., Vieira, G., Palacios, D., Garcia-Oteyza, J., Ventura, J., Schimmelpfennig, I., ASTER Team, 2023. Geomorphological record of the glacial to periglacial transition from the Bølling–Allerød to the Holocene in the Central Pyrenees: the Lòcampo cirque in the regional context. Boreas. https://doi.org/10.1111/bor.12633

Ffoulkes, C., Harrison, S., 2014. Evaluating the Schmidt hammer as a method for distinguishing the relative age of late Holocene moraines: Svellnosbreen, Jotunheimen, Norway. Geogr. Ann. Ser. A, Phys. Geogr. 96 (3), 393–402. https://doi.org/10.1111/geoa.12055

Frauenfelder, R., Laustela, M., Kääb, A., 2005. Relative age dating of Alpine rockglacier surfaces. Zeitschrift für Geomorphol. 49 (2), 145–166.

Frochoso, M., González-Pellejero, R., Allende, F., 2013. Pleistocene glacial morphology and timing of last glacial cycle in Cantabrian Mountains (Northern

Spain): New chronological data from the Asón area. Cent. Eur. J. Geosci. 5 (1), 12–27. https://doi.org/10.2478/s13533-012-0117-8

García-Ruiz, J.M., Valero-Garcés, B.L., Martí-Bono, C., González-Sampériz, P., 2003. Asynchroneity of maximum glacier advances in the central Spanish Pyrenees. Journal of Quaternary Science, 18 (1), 61-72. https://doi.org/10.1002/jqs.715

García-Ruiz, J.M., Palacios, D., Fernández-Fernández, J.M., Andrés, N., Arnáez, J., Gómez-Villar, A., Santos-González, J., Álvarez-Martínez, J., Lana-Renault, N., Léanni, L., 2020. Glacial stages in the Peña Negra valley, Iberian Range, northern Iberian Peninsula: Assessing the importance of the glacial record in small cirques in a marginal mountain area. Geomorphology 107195. https://doi.org/10.1016/j.geomorph.2020.107195

García de Celis, A., 1991. Los glaciares rocosos de la Sierra del Suspirón (León). Polígonos 1, 9–20. https://doi.org/10.18002/pol.v0i1.567

García de Celis, A., 2002. Formas periglaciares relictas en la Sierra del Suspirón (Cordillera Cantábrica, León): campos de bloques, in: Serrano, E., García de Celis, A. (Eds.), Periglaciarismo en montaña y altas latitudes. Universidad de Valladolid, Valladolid, pp. 37–52.

García de Celis, A., Martínez Fernández, L.C., 2002. Morfología glaciar de las montañas de la cuenca alta de los ríos Sil, Omaña, Luna y Bernesga: revisión y nuevos datos (Montaña Occidental de León), in: Redondo Vega, J.M., Gómez Villar, A., González Gutiérrez, R.B., Carrera Gómez, P. (Eds.), El modelado de origen glaciar en las Montañas Leonesas. Universidad de León, León, pp. 137–196.

Goehring, B.M., Brook, E.J., Linge, H., Raisbeck, G.M., Yiou, F., 2008. Beryllium-10 exposure ages of erratic boulders in southern Norway and implications for the history of the Fennoscandian Ice Sheet. Quat. Sci. Rev. 27 (3), 320–336.

https://doi.org/10.1016/j.quascirev.2007.11.004

Gómez-Villar, A., González-Gutiérrez, R.B., Redondo-Vega, J.M., Santos-González, J., 2011. Distribución de glaciares rocosos relictos en la cordillera cantábrica. Cuad. Investig. Geogr. 37 (2), 49–80. https://doi.org/10.18172/cig.1256

González-Gutiérrez, R.B., Santos-González, J., Gómez-Villar, A., Redondo-Vega, J.M., 2019. Surface macro-fabric analysis of relict rock glaciers in the Cantabrian Mountains (NW Spain). Permafr. Periglac. Process. 30 (4), 348–363. https://doi.org/10.1002/ppp.2025

González Trueba, J.J., Moreno, R.M., Martínez De Pisón, E., Serrano, E., 2008. "Little ice age" glaciation and current glaciers in the Iberian Peninsula. Holocene 18 (4), 551–568. https://doi.org/10.1177/0959683608089209

Goodfellow, B.W., Stroeven, A.P., Fabel, D., Fredin, O., Derron, M.-H., Bintanja, R., Caffee, M.W., 2014. Arctic–alpine blockfields in the northern Swedish Scandes: late Quaternary – not Neogene. Earth Surf. Dyn. 2 (2), 383–401. https://doi.org/10.5194/esurf-2-383-2014

Goudie, A.S., 2006. The Schmidt Hammer in geomorphologial research. Prog. Phys. Geogr. 30 (6), 703–718 https://doi.org/10.1177/0309133306071954

Guglielmin, M., Worland, M.R., Convey, P., Cannone, N., 2012. Schmidt Hammer studies in the maritime Antarctic: Application to dating Holocene deglaciation and estimating the effects of macrolichens on rock weathering. Geomorphology 155–156, 34–44. https://doi.org/10.1016/j.geomorph.2011.12.015

Hopkinson, C., Ballantyne, C.K., 2014. Age and Origin of Blockfields on Scottish Mountains. Scottish Geogr. J. 130, 116–141. https://doi.org/10.1080/14702541.2013.855808

Hughes, P.D., 2022. The glacial landscapes of the Iberian Peninsula within the

Mediterranean Region, in: Oliva, M., Palacios, D., Fernández-Fernández, J.M. (Eds.), Iberia, Land of Glaciers. Elsevier, pp. 37-54. https://doi.org/10.1016/B978-0-12-821941-6.00003-7

Hughes, P.D., Woodward, J.C., 2008. Timing of glaciation in the Mediterranean mountains during the last cold stage. J Quat Sci., 23 (6-7), 575-588. https://doi.org/10.1002/jqs.1212

Hughes, P., Tomkins, M., Stimson, A., 2019. Glaciation of the English Lake District during the Late-glacial: a new analysis using 10Be and Schmidt hammer exposure dating. Northwest Geography, 19 (2), 8-20. https://www.mangeogsoc.org.uk/pdfs/hughes_19_2.pdf

Jalut, G., Turu i Michels, V., Dedoubat, J.J., Otto, T., Ezquerra, J., Fontugne, M., Belet, J.M., Bonnet, L., García de Celis, A., Redondo-Vega, J.M., Vidal-Romaní, J.R., Santos, L., 2010. Palaeoenvironmental studies in NW Iberia (Cantabrian range): Vegetation history and synthetic approach of the last deglaciation phases in the western Mediterranean. Palaeogeogr. Palaeoclimatol. Palaeoecol. 297 (2), 330–350. https://doi.org/10.1016/j.palaeo.2010.08.012

Jiménez-Sánchez, M., Rodríguez-Rodríguez, L., González-Lemos, S., Domínguez-Cuesta, M.J., 2022. The glaciers in the Redes Natural Park, in: Oliva, M., Palacios, D., Fernández-Fernández, J.M. (Eds.), Iberia, Land of Glaciers. Elsevier, pp. 221–235. https://doi.org/10.1016/B978-0-12-821941-6.00011-6

Kellerer-Pirklbauer, A., Wangensteen, B., Farbrot, H., Etzelmüller, B., 2008. Relative surface age-dating of rock glacier systems near Hólar in Hjaltadalur, northern Iceland. J. Quat. Sci. 23 (2), 137–151. https://doi.org/10.1002/jqs.1117

Kłapyta, P., 2013. Application of Schmidt hammer relative age dating to Late Pleistocene moraines and rock glaciers in the Western Tatra Mountains, Slovakia.

Catena 111, 104–121. https://doi.org/10.1016/j.catena.2013.07.004

Linge, H., Nesje, A., Matthews, J.A., Fabel, D., Xu, S., 2020. Evidence for rapid paraglacial formation of rock glaciers in southern Norway from 10 Be surface-exposure dating. Quat. Res. 97, 55–70. https://doi.org/10.1017/qua.2020.10

Marr, P., Winkler, S., Löffler, J., 2018. Investigations on blockfields and related landforms at Blåhø (Southern Norway) using Schmidt-hammer exposure-age dating: palaeoclimatic and morphodynamic implications. Geogr. Ann. Ser. A, Phys. Geogr. 100 (1), 285–306. https://doi.org/10.1080/04353676.2018.1474350

Marr, P., Winkler, S., Löffler, J., 2019. Schmidt-hammer exposure-age dating (SHD) performed on periglacial and related landforms in Opplendskedalen, Geirangerfjellet, Norway: Implications for mid- and late-Holocene climate variability. Holocene 29 (1), 97-109. https://doi.org/10.1177/0959683618804634

Marr, P., Winkler, S., Dahl, S.O., Löffler, J., 2022. Age, origin and palaeoclimatic implications of peri- and paraglacial boulder-dominated landforms in Rondane, South Norway. Geomorphology 408, 108251. https://doi.org/10.1016/j.geomorph.2022.108251

Martínez-Fernández, A., Serrano, E., Sanjosé, J.J., Gómez-Lende, M., Pisabarro, A., Sánchez, M., 2019. Geomatic methods applied to the change study of the La Paúl rock glacier, Spanish Pyrenees. International Archives of the Photogrammetry, Remote Sensing and Spatial Information Sciences - ISPRS Archives, 42(2/W13). https://doi.org/10.5194/isprs-archives-XLII-2-W13-1771-2019

Matthews, J.A., Winkler, S., 2022. Schmidt-hammer exposure-age dating: a review of principles and practice. Earth-Science Rev. 230, 104038. https://doi.org/10.1016/j.earscirev.2022.104038

Matthews, J.A., Shakesby, R.A., Owen, G., Vater, A.E., 2011. Pronival rampart

formation in relation to snow-avalanche activity and Schmidt-hammer exposure-age dating (SHD): Three case studies from southern Norway. Geomorphology 130 (3-4), 280–288. https://doi.org/10.1016/j.geomorph.2011.04.010

Matthews, J.A., Nesje, A., Linge, H., 2013. Relict Talus-Foot Rock Glaciers at Øyberget, Upper Ottadalen, Southern Norway: Schmidt Hammer Exposure Ages and Palaeoenvironmental Implications. Permafr. Periglac. Process. 24 (4), 336–346. https://doi.org/10.1002/ppp.1794

Matthews, J.A., McEwen, L.J., Owen, G., 2015. Schmidt-hammer exposure-age dating (SHD) of snow-avalanche impact ramparts in southern Norway: approaches, results and implications for landform age, dynamics and development. Earth Surf. Process. Landforms 40 (13), 1705–1718. https://doi.org/10.1002/esp.3746

Matthews, J.A., Winkler, S., Wilson, P., 2014. Age and origin of ice-cored moraines in Jotunheimen and Breheimen, southern Norway: insights from Schmidt-hammer exposure-age dating. Geogr. Ann. Ser. A, Phys. Geogr. 96 (4), 531-548. https://doi.org/10.1111/geoa.12046

Matthews, J.A., Linge, H., Nesje, A., Wilson, P., Mourne, R.W., Winkler, S., Owen, G., Hill, J.L., Haselberger, S., Olsen, J., 2023. Deglaciation of the highest mountains in Scandinavia at the Younger Dryas–Holocene transition: evidence from surface exposure-age dating of ice-marginal moraines. Boreas. https://doi.org/10.1111/bor.12644

McCarroll, D., Nesje, A., 1993. The vertical extent of ice sheets in Nordfjord, western Norway: measuring degree of rock surface weathering. Boreas 22 (3), 255–265. https://doi.org/10.1111/j.1502-3885.1993.tb00185.x

Melón-Nava, A., Santos-González, J., María Redondo-Vega, J., Blanca González-Gutiérrez, R., Gómez-Villar, A., 2022. Factors influencing the ground thermal

regime in a mid-latitude glacial cirque (Hoyo Empedrado, Cantabrian Mountains, 2006–2020). Catena 212, 106110. https://doi.org/10.1016/j.catena.2022.106110

Moreno, A., Valero-Garcés, B.L., Jiménez-Sánchez, M., Domínguez-Cuesta, M.J., Mata, M.P., Navas, A., González-Sampériz, P., Stoll, H., Farias, P., Morellón, M., Corella, J.P., Rico, M., 2010. The last deglaciation in the Picos de Europa National Park (Cantabrian Mountains, northern Spain). J. Quat. Sci. 25 (7), 1076–1091. https://doi.org/10.1002/jqs.1265

Nesje, A., Matthews, J.A., Linge, H., Bredal, M., Wilson, P., Winkler, S., 2021. New evidence for active talus-foot rock glaciers at Øyberget, southern Norway, and their development during the Holocene. The Holocene, 31 (11-12), 1786-1796. https://doi.org/10.1177/09596836211033226

Oliva, M., Serrano, E., Gómez-Ortiz, A., González-Amuchastegui, M.J., Nieuwendam, A., Palacios, D., Pérez-Alberti, A., Pellitero-Ondicol, R., Ruiz-Fernández, J., Valcárcel, M., Vieira, G., Antoniades, D., 2016. Spatial and temporal variability of periglaciation of the Iberian Peninsula. Quat. Sci. Rev. 137, 176–199. https://doi.org/10.1016/j.quascirev.2016.02.017

Oliva, Marc, Serrano, E., Fernández-Fernández, José M., Palacios, D., Fernandes, M., García-Ruiz, J.M., López-Moreno, J.I., Pérez-Alberti, A., Antoniades, D., 2022. The Iberian Peninsula, in: Oliva, M., Nývlt, D., Fernández-Fernández, J.M. (Eds.), Periglacial Landscapes of Europe. Springer International Publishing, Cham, pp. 43–68. https://doi.org/10.1007/978-3-031-14895-8_4

Oliva, M., Andrés, Nuria, Fernández-Fernández, J.M., Palacios, David, 2023a. The evolution of glacial landforms in the Iberian Mountains during the Bølling–Allerød Interstadial, in: Palacios, D., Hughes, P.D., García-Ruiz, J.M., Andrés, N. (Eds.), European Glacial Landscapes. The Last Deglaciation. Elsevier, pp. 369–377.

https://doi.org/10.1016/B978-0-323-91899-2.00013-9

Oliva, M., Andrés, Nuria, Fernández-Fernández, J.M., Palacios, David, 2023b. The evolution of glacial landforms in the Iberian Mountains during the Younger Dryas Stadial, in: Palacios, D., Hughes, P.D., García-Ruiz, J.M., Andrés, N. (Eds.), European Glacial Landscapes. The Last Deglaciation. Elsevier, pp. 553–562. https://doi.org/10.1016/B978-0-323-91899-2.00037-1

Onaca, A., Ardelean, F., Urdea, P., Magori, B., 2017. Southern Carpathian rock glaciers: Inventory, distribution and environmental controlling factors. Geomorphology 293 (part B), 391–404. https://doi.org/10.1016/j.geomorph.2016.03.032

Otto J, Kahle D., 2023. ggdensity: Interpretable Bivariate Density Visualization with 'ggplot2'. https://jamesotto852.github.io/ggdensity/

Owen, G., Matthews, J.A., Albert, P.G., 2007. Rates of Holocene chemical weathering, `Little Ice Age' glacial erosion and implications for Schmidt-hammer dating at a glacier—foreland boundary, Fåbergstølsbreen, southern Norway. The Holocene 17 (6), 829–834. https://doi.org/10.1177/0959683607081419

Palacios, D., de Andrés, N., de Marcos, J., Vázquez-Selem, L., 2012. Glacial landforms and their paleoclimatic significance in Sierra de Guadarrama, Central Iberian Peninsula. Geomorphology 139–140, 67–78. https://doi.org/10.1016/j.geomorph.2011.10.003

Palacios, D., Gómez-Ortiz, A., Andrés, N., Vázquez-Selem, L., Salvador-Franch, F., Oliva, M., 2015. Maximum extent of Late Pleistocene glaciers and last deglaciation of La Cerdanya mountains, Southeastern Pyrenees. Geomorphology 231, 116–129. https://doi.org/10.1016/j.geomorph.2014.10.037

Palacios, D., García-Ruiz, J.M., Andrés, N., Schimmelpfennig, I., Campos, N., Léanni, L., ASTER Team, 2017. Deglaciation in the central Pyrenees during the

Pleistocene–Holocene transition: Timing and geomorphological significance. Quat. Sci. Rev. 162. https://doi.org/10.1016/j.quascirev.2017.03.007

Palacios, D., Rodríguez-Mena, M., Fernández-Fernández, J.M., Schimmelpfennig, I., Tanarro, L.M., Zamorano, J.J., Andrés, N., Úbeda, J., Sæmundsson, Þ., Brynjólfsson, S., Oliva, M., Team, A., 2021. Reversible glacial-periglacial transition in response to climate changes and paraglacial dynamics: a case study from Héðinsdalsjökull (northern Iceland). Geomorphology 388, 107787. https://doi.org/10.1016/j.geomorph.2021.107787

Pellitero, R., 2009. Application of an alpine geomorphological mapping system to an atlantic mountain environment: The Curavacas Massif (Cantabrian Range, Northwest Spain). J. Maps 5 (1), 194–205. https://doi.org/10.4113/jom.2009.1065

Pellitero, R., 2014. Geomorphology and geomorphological landscapes of Fuentes Carrionas. J. Maps 10 (2), 313–323. https://doi.org/10.1080/17445647.2013.867822

Pellitero, R., 2022. The glaciers of the Montaña Palentina, in: Oliva, M., Palacios, D., Fernández-Fernández, J.M. (Eds.), Iberia, Land of Glaciers. Elsevier, pp. 179–199. https://doi.org/10.1016/B978-0-12-821941-6.00009-8

Pellitero, R., Serrano, E., González Trueba, J.J., 2011. Glaciares rocosos del sector central de la montaña cantábrica: Indicadores paleoambientales. Cuad. Investig. Geogr. 37 (2), 119–144. https://doi.org/10.18172/cig.1259

Pellitero, R., Fernández-Fernández, J.M., Campos, N., Serrano, E., Pisabarro, A., 2019. Late Pleistocene climate of the northern Iberian Peninsula: New insights from palaeoglaciers at Fuentes Carrionas (Cantabrian Mountains). J. Quat. Sci. 34 (4-5), 342–354. https://doi.org/10.1002/jqs.3106

Peña-Pérez, S., 2021. Rasgos morfométricos de los canchales y sus áreas fuente de la

vertiente occidental del macizo de Las Ubiñas (cordillera Cantábrica, León). Cuaternario y Geomorfol. 35 (3-4), 175-190. https://doi.org/10.17735/cyg.v35i3-4.89830

Pérez Alberti, A., Rodríguez Guitián, M., 1993. Formas y depósitos de macroclastos y manifestaciones actuales de periglaciarismo en las sierras septentrionales y orientales de Galicia, in: Pérez Alberti, A., Guitián Rivera, L., Ramil Rego, P. (Eds), La evolución del paisaje en las montañas del entorno de los Caminos Jacobeos: cambios ambientales y actividad humana. Junta de Galicia, pp. 91-105.

Pérez-Alberti, A., Valcarcel, M., 2022. The glaciers in Eastern Galicia, in: Oliva, M., Palacios, D., Fernández-Fernández, J.M. (Eds.), Iberia, Land of Glaciers. Elsevier, pp. 375–395. https://doi.org/10.1016/B978-0-12-821941-6.00018-9

Pisabarro, A., Pellitero, R., Serrano, E., Gómez-Lende, M., González-Trueba, J.J., 2017. Ground temperatures, landforms and processes in an Atlantic mountain. Cantabrian Mountains (Northern Spain). Catena 149 (2), 623–636. https://doi.org/10.1016/j.catena.2016.07.051

Prado, C., 1852. Notes sur les blocs erratiques de la Chaine Cantabrique. Bulletin Societè Geologique de France, 9, 171-175.

Rae, A.C., Harrison, S., Mighall, T., Dawson, A.G., 2004. Periglacial trimlines and nunataks of the Last Glacial Maximum: the Gap of Dunloe, southwest Ireland. J. Quat. Sci. 19 (1), 87–97. https://doi.org/10.1002/jqs.807

R Core Team, 2022. R: A language and environment for statistical computing. R Foundation for Statistical Computing, Vienna, Austria. URL. https://www.R-project.org/

Redondo-Vega, J.M., Gómez-Villar, A., González-Gutiérrez, R.B., 1998. Los glaciares rocosos fósiles de la Sierra de Gistredo (Montaña Cantábrica, León), in: Gómez-

Ortiz, A., Salvador-Franch, F. (Eds.), Investigaciones recientes de la geomorfología española. Universitat de Barcelona, Barcelona, pp. 745–750.

Redondo Vega, J.M., Gómez Villar, A., González Gutiérrez, R.B., Carrera Gómez, P. 2002a. Caracterización de los macizos que dominan los glaciares rocosos fósiles de la Sierra de Gistredo (León): Influencia de la fracturación en la génesis y desarrollo de estas formas periglaciares, in: Serrano, E., García de Celis, A. (Eds.), Periglaciarismo en Montaña y altas latitudes. Universidad de Valladolid, Valladolid, pp. 27-36.

Redondo Vega, J.M., Gómez Villar, A., González Gutiérrez, R.B., Carrera Gómez, P., 2002b. El relieve glaciar del macizo del Vizcodillo, Cabrera Alta, León, in: Redondo Vega, J.M., Gómez Villar, A., González Gutiérrez, R.B., Carrera Gómez, P. (Eds.), El modelado de origen glaciar en las montañas leonesas. Universidad de León, León, pp. 13–28.

Redondo-Vega, J.M., Gómez-Villar, A., González-Gutiérrez, R.B., Santos-González, J., 2010. Los glaciares rocosos de la Cordillera Cantábrica. Universidad de León, León.

Redondo-Vega, J.M., Alonso Herrero, E., García de Celis, A., Gómez Villar, A., González Gutiérrez, R.B., Santos González, J., 2014. Huellas glaciares a baja altitud en los valles cantábricos meridionales, in: Geoecología, Cambio ambiental y Paisaje: Homenaje Al Profesor José María García Ruiz. pp. 103–116.

Redondo-Vega, J.M., Santos-González, J., González-Gutiérrez, R.B., Gómez-Villar, A., 2022. The glaciers of the Montes de León, in: Oliva, M., Palacios, D., Fernández-Fernández, J.M. (Eds.), Iberia, Land of Glaciers. Elsevier, pp. 315–333. https://doi.org/10.1016/B978-0-12-821941-6.00015-3

Rode, M., Kellerer-Pirklbauer, A., 2012. Schmidt-hammer exposure-age dating (SHD)

of rock glaciers in the Schöderkogel-Eisenhut area, Schladminger Tauern Range, Austria. The Holocene 22 (7), 761–771. https://doi.org/10.1177/0959683611430410

Rodríguez-Rodríguez, L., Jiménez-Sánchez, M., Domínguez-Cuesta, M.J., Rinterknecht, V., Pallàs, R., Bourlès, D., 2016. Chronology of glaciations in the Cantabrian Mountains (NW Iberia) during the Last Glacial Cycle based on in situ-produced 10Be. Quat. Sci. Rev. 138, 31–48. https://doi.org/10.1016/j.quascirev.2016.02.027

Rodríguez-Rodríguez, L., Jiménez-Sánchez, M., Domínguez-Cuesta, M.J., Rinterknecht, V., Pallàs, R., ASTER Team, 2017. Timing of last deglaciation in the Cantabrian Mountains (Iberian Peninsula; North Atlantic Region) based on in situ-produced 10Be exposure dating. Quat. Sci. Rev. 171, 166–181. https://doi.org/10.1016/j.quascirev.2017.07.012

Rodríguez-Rodríguez, L., Domínguez-Cuesta, M.J., Rinterknecht, V., Jiménez-Sánchez, M., González-Lemos, S., Léanni, L., Sanjurjo, J., Ballesteros, D., Valenzuela, P., Llana-Fúnez, S., 2018. Constraining the age of superimposed glacial records in mountain environments with multiple dating methods (Cantabrian Mountains, Iberian Peninsula). Quat. Sci. Rev. 195, 215–231. https://doi.org/10.1016/j.quascirev.2018.07.025

Rodríguez-Rodríguez, L., Jiménez-Sánchez, M., Domínguez-Cuesta, M.J., González-Lemos, S., 2022. The glaciers around Lake Sanabria, in: Oliva, M., Palacios, D., Fernández-Fernández, J.M. (Eds.), Iberia, Land of Glaciers. Elsevier, pp. 335–351. https://doi.org/10.1016/B978-0-12-821941-6.00016-5

Rodríguez, C., Sevilla, J., Obeso, Í., Herrera, D., 2022. Emerging Tools for the Interpretation of Glacial and Periglacial Landscapes with Geomorphological Interest—A Case Study Using Augmented Reality in the Mountain Pass of San

Isidro (Cantabrian Range, Northwestern Spain). Land 11 (8), 1327. https://doi.org/10.3390/land11081327

Rodríguez Pérez, C., 1995. Estudio geomorfológico del puerto de San Isidro. Ería 36, 63–87. https://doi.org/10.17811/er.0.1995.63-87

Ruiz-Fernández, J., Oliva, M., Cruces, A., Lopes, V., Freitas, M.C., Andrade, C., García-Hernández, C., López-Sáez, J.A., Geraldes, M., 2016. Environmental evolution in the Picos de Europa (Cantabrian Mountains, SW Europe) since the Last Glaciation. Quat. Sci. Rev. 138, 87-104. https://doi.org/10.1016/j.quascirev.2016.03.002

Ruiz-Fernández, J., García-Hernández, C., Gallinar Cañedo, D., 2022a. The glaciers of the Picos de Europa, in: Iberia, Land of Glaciers. Elsevier, pp. 237–263. https://doi.org/10.1016/B978-0-12-821941-6.00012-8

Ruiz-Fernández, J., González-Díaz, B., Cañedo, D.G., García-Hernández, C., 2022b. The glaciers of the Central-Western Asturian Mountains, in: Oliva, M., Palacios, D., Fernández-Fernández, J.M. (Eds.), Iberia, Land of Glaciers. Elsevier, pp. 265–288. https://doi.org/10.1016/B978-0-12-821941-6.00013-X

Santos González, J., 2011. Glaciarismo y periglaciarismo en el Alto Sil, provincia de León (Cordillera Cantábrica). Universidad de León.

Santos-González, J., Redondo-Vega, J.M., González-Gutiérrez, R.B., Gómez-Villar, A., 2013. Applying the AABR method to reconstruct equilibrium-line altitudes from the last glacial maximum in the Cantabrian Mountains (SW Europe). Palaeogeogr. Palaeoclimatol. Palaeoecol. 387, 185–199. https://doi.org/10.1016/j.palaeo.2013.07.025

Santos-González, J., González-Gutiérrez, R.B., Redondo-Vega, J.M., Gómez-Villar, A., 2016. Distribución y caracterización de bloques aradores en el noroeste de la

Península Ibérica: el Alto Sil y el Macizo de Vizcodillo. Polígonos. Rev. Geogr. 139–159. https://doi.org/10.18002/pol.v0i28.4291

Santos-González, J., González-Gutiérrez, R.B., Santos, J.A., Gómez-Villar, A., Peña-Pérez, S.A., Redondo-Vega, J.M., 2018. Topographic, lithologic and glaciation style influences on paraglacial processes in the upper Sil and Luna catchments, Cantabrian Mountains, NW Spain. Geomorphology 319, 133–146. https://doi.org/10.1016/j.geomorph.2018.07.019

Santos-González, J., González-Gutiérrez, R.B., Redondo-Vega, J.M., Gómez-Villar, A., Jomelli, V., Fernández-Fernández, J.M., Andrés, N., García-Ruiz, J.M., Peña-Pérez, S.A., Melón-Nava, A., Oliva, M., Álvarez-Martínez, J., Charton, J., Palacios, D., 2022a. The origin and collapse of rock glaciers during the Bølling-Allerød interstadial: A new study case from the Cantabrian Mountains (Spain). Geomorphology 401, 108112. https://doi.org/10.1016/j.geomorph.2022.108112

Santos-González, J., Redondo-Vega, J.M., Celis, A.G., González-Gutiérrez, R.B., Gómez-Villar, A., 2022b. The glaciers of the Leonese Cantabrian Mountains, in: Oliva, M., Palacios, D., Fernández-Fernández, J.M. (Eds.), Iberia, Land of Glaciers. Elsevier, pp. 289–314. https://doi.org/10.1016/B978-0-12-821941-6.00014-1

Scapozza, C., Del Siro, C., Lambiel, C., Ambrosi, C., 2021. Schmidt hammer exposure-age dating of periglacial and glacial landforms in the Southern Swiss Alps based on R-value calibration using historical data. Geogr. Helv. 76 (4), 401–423. https://doi.org/10.5194/gh-76-401-2021

Scapozza, C., Lambiel, C., Bozzini, C., Mari, S., Conedera, M., 2014. Assessing the rock glacier kinematics on three different timescales: a case study from the southern Swiss Alps. Earth Surf. Process. Landforms 39 (15), 2056–2069. https://doi.org/10.1002/esp.3599

Schmitz, H., 1969. Glazialmorphologische Untersuchungen Im Bergland Nordwestspaniens (Galicie-León). Kölner Geographische Arbeiten, 23.

Serrano, E., 2014. Glaciares rocosos. Controversias y certidumbres, in: Gómez-Ortiz, A., Salvador-Franch, F., Oliva, M., Salvà, M. (Eds.), Avances, métodos y técnicas en el estudio del periglaciarismo. Universitat de Barcelona, Barcelona, pp. 115–134.

Serrano E., Sanjosé, J.J., González Trueba, J.J. 2010. Rock glaciers dynamics in marginal periglacial environments. Earth Surf. Process. Landforms 35, 1302–1314. https://doi.org/10.1002/esp.1972

Serrano, E., González-Trueba, J.J., González-García, M., 2012. Mountain glaciation and paleoclimate reconstruction in the Picos de Europa (Iberian Peninsula, SW Europe). Quat. Res. 78 (2), 303–314. https://doi.org/10.1016/j.yqres.2012.05.016

Serrano, E., González-Trueba, J.J., Pellitero, R., González-García, M., Gómez-Lende, M., 2013. Quaternary glacial evolution in the Central Cantabrian Mountains (Northern Spain). Geomorphology 196, 65–82. https://doi.org/10.1016/j.geomorph.2012.05.001

Serrano, E., Gómez-Lende, M., Pellitero, R., González Trueba, J.J., 2015. Deglaciation in the Cantabrian Mountains: pattern and evolution. Cuad. Investig. Geográfica 41 (2), 389. https://doi.org/10.18172/cig.2716

Serrano, E., González-Trueba, J.J., Pellitero, R., Gómez-Lende, M., 2017. Quaternary glacial history of the Cantabrian Mountains of northern Spain: A new synthesis, in: Geological Society Special Publication. pp. 55–85. https://doi.org/10.1144/SP433.8

Serrano, E., Oliva, M., González-García, M., López-Moreno, J.I., González-Trueba, J., Martín-Moreno, R., Gómez-Lende, M., Martín-Díaz, J., Nofre, J., Palma, P., 2018. Post-little ice age paraglacial processes and landforms in the high Iberian

mountains: A review. L. Degrad. Dev. 29 (11), 4186–4208. https://doi.org/10.1002/ldr.3171

Serrano, E., Gómez-Lende, M., González-Amuchastegui, M.J., 2022a. The glaciers of the eastern massifs of Cantabria, the Burgos Mountains and the Basque Country, in: Oliva, M., Palacios, D., Fernández-Fernández, J.M. (Eds.), Iberia, Land of Glaciers. Elsevier, pp. 157–178. https://doi.org/10.1016/B978-0-12-821941-6.00008-6

Serrano, E., Gómez-Lende, M., Pisabarro, A., 2022b. The glaciers of the western massifs of Cantabria, in: Oliva, M., Palacios, D., Fernández-Fernández, J.M. (Eds.), Iberia, Land of Glaciers. Elsevier, pp. 201–219. https://doi.org/10.1016/B978-0-12-821941-6.00010-4

Shakesby, R.A., Dawson, A.G., Matthews, J.A., 1987. Rock glaciers, protalus ramparts and related phenomena, Rondane, Norway: a continuum of large-scale talus-derived landforms. Boreas 16 (3), 305–317. https://doi.org/10.1111/j.1502-3885.1987.tb00099.x

Shakesby, R.A., Matthews, J.A., Winkler, S., 2004. Glacier variations in Breheimen, southern Norway: relative-age dating of Holocene moraine complexes at six high-altitude glaciers. The Holocene 14 (6), 899–910. https://doi.org/10.1191/0959683603hl766rp

Shakesby, R.A., Matthews, J.A., Owen, G., 2006. The Schmidt hammer as a relative-age dating tool and its potential for calibrated-age dating in Holocene glaciated environments. Quat. Sci. Rev. 25 (21), 2846–2867. https://doi.org/10.1016/j.quascirev.2006.07.011

Shakesby, R.A., Matthews, J.A., Karlén, W., Los, S.O., 2011. The Schmidt hammer as a Holocene calibrated-age dating technique: Testing the form of the R-value-age relationship and defining the predicted-age errors. The Holocene 21 (4), 615–628.

https://doi.org/10.1177/0959683610391322

Stickel, R., 1929. Observaciones de morfología glaciar en el NO. de España. Boletín la Real Soc. Española Hist. Nat. 29, 297–313.

Tanarro, L.M., Palacios, D., Fernández-Fernández, J.M., Andrés, N., Oliva, M., Rodríguez-Mena, M., Schimmelpfennig, I., Brynjólfsson, S., Sæmundsson, Þ., Zamorano, J.J., Úbeda, J., Aumaître, G., Bourlès, D., Keddadouche, K., 2021. Origins of the divergent evolution of mountain glaciers during deglaciation: Hofsdalur cirques, Northern Iceland. Quat. Sci. Rev. 273, 107248. https://doi.org/10.1016/j.quascirev.2021.107248

Tomkins, M.D., Dortch, J.M., Hughes, P.D., 2016. Schmidt Hammer exposure dating (SHED): Establishment and implications for the retreat of the last British Ice Sheet. Quat. Geochronol. 33, 46–60. https://doi.org/10.1016/j.quageo.2016.02.002

Tomkins, M.D., Dortch, J.M., Hughes, P.D., Huck, J.J., Stimson, A.G., Delmas, M., Calvet, M., Pallàs, R., 2018a. Rapid age assessment of glacial landforms in the Pyrenees using Schmidt hammer exposure dating (SHED). Quat. Res. 90 (1). https://doi.org/10.1017/qua.2018.12

Tomkins, M.D., Huck, J.J., Dortch, J.M., Hughes, P.D., Kirbride, M.P., Barr, I.D., 2018b. Schmidt Hammer exposure dating (SHED): Calibration procedures, new exposure age data and an online calculator. Quat. Geochronol. 44 https://doi.org/10.1016/j.quageo.2017.12.003

Tonkin, T.N., 2022. Schmidt Hammer exposure-age dating of glacial landforms in the Cairngorm Mountains, Scotland. Zeitschrift für Geomorphol. 64 (1), 39–52. https://doi.org/10.1127/zfg/2022/0756

Valcárcel-Díaz, M., Pérez-Alberti, A., 2002. Los campos de bloques en montañas del noroeste de la Península Ibérica: génesis y significado paleoambiental, in: Serrano,

E., García de Celis, A. (Eds.), Periglaciarismo en montaña y altas latitudes. Universidad de Valladolid, Valladolid, pp. 13–26.

Viana-Soto, A., Pérez-Alberti, A., 2019. Periglacial deposits as indicators of paleotemperatures. A case study in the Iberian Peninsula: The mountains of Galicia. Permafr. Periglac. Process. 30 (4), 374–388. https://doi.org/10.1002/ppp.2026

Viles, H., Goudie, A., Grab, S., Lalley, J., 2011. The use of the Schmidt Hammer and Equotip for rock hardness assessment in geomorphology and heritage science: a comparative analysis. Earth Surf. Process. Landforms 36 (3), 320–333. https://doi.org/10.1002/esp.2040

Wickham, H., 2016. ggplot2: Elegant Graphics for Data Analysis. Springer-Verlag New York. ISBN 978-3-319-24277-4. https://ggplot2.tidyverse.org

Wilson, P., Matthews, J.A., 2016. Age assessment and implications of late Quaternary periglacial and paraglacial landforms on Muckish Mountain, northwest Ireland, based on Schmidt-hammer exposure-age dating (SHD). Geomorphology 270, 134–144. https://doi.org/10.1016/j.geomorph.2016.07.002

Wilson, P., Matthews, J.A., Mourne, R.W., 2017. Relict Blockstreams at Insteheia, Valldalen-Tafjorden, Southern Norway: Their Nature and Schmidt Hammer Exposure Age. Permafr. Periglac. Process. 28 (1), 286–297. https://doi.org/10.1002/ppp.1915

Wilson, P., Dunlop, P., Millar, C., Wilson, F.A., 2019a. Age determination of glacially-transported boulders in Ireland and Scotland using Schmidt-hammer exposure-age dating (SHD) and terrestrial cosmogenic nuclide (TCN) exposure-age dating. Quat. Res. 92, 570–582. https://doi.org/10.1017/qua.2019.12

Wilson, P., Linge, H., Matthews, J.A., Mourne, R.W., Olsen, J., 2019b. Comparative numerical surface exposure-age dating (10 Be and Schmidt hammer) of an early-

Holocene rock avalanche at Alstadfjellet, Valldalen, southern Norway. Geogr. Ann. Ser. A, Phys. Geogr. 101 (4), 293–309. https://doi.org/10.1080/04353676.2019.1644815

Winkler, S., 2005. The Schmidt hammer as a relative-age dating technique: Potential and limitations of its application on Holocene moraines in Mt Cook National Park, Southern Alps, New Zealand. New Zeal. J. Geol. Geophys. 48 (1), 105–116. https://doi.org/10.1080/00288306.2005.9515102

Winkler, S., 2022. Schmidt-hammer exposure-age dating (SHD) of periglacial landforms and its potential for palaeoclimatic and morphodynamic interpretation, in: IAG (Ed.), 10th International Conference on Geomorphology. Coimbra (Portugal). https://doi.org/https://doi.org/10.5194/icg2022-3

Winkler, S., Lambiel, C., 2018. Age constraints of rock glaciers in the Southern Alps/New Zealand – Exploring their palaeoclimatic potential. The Holocene 28 (5), 778-790. https://doi.org/10.1177/0959683618756802

Winkler, S., Matthews, J.A., Shakesby, R.A., Dresser, P.Q., 2003. Glacier variations in Breheimen, southern Norway: dating Little Ice Age moraine sequences at seven low-altitude glaciers. J. Quat. Sci. 18 (5), 395–413. https://doi.org/10.1002/jqs.756

Winkler, S., Matthews, J.A., Haselberger, S., Hill, J.L., Mourne, R.W., Owen, G., Wilson, P., 2020. Schmidt-hammer exposure-age dating (SHD) of sorted stripes on Juvflye, Jotunheimen (central South Norway): Morphodynamic and palaeoclimatic implications. Geomorphology 107014. https://doi.org/10.1016/j.geomorph.2019.107014

Table 1. Location, geomorphological units, and number of impacts for each of the sampled sites

Area	Lithology	Landform	Sample	Altitude (m a.s.l.)	X[1]	Y[1]	Impacts
Arcos del Agua	Quartzite (Cabos Series)	Lower Rock glacier	AR-01	1619	726696	4741779	120
			AR-02	1690	726545	4741599	120
			AR-03	1700	726487	4741532	120
		Talus slopes	AR-04	1751	726445	4741385	120
			AR-05	1783	726479	4741266	120
			AR-06	1783	726455	4741270	120
			AR-07	1829	726472	4741137	120
		Blockfield	AR-08	1997	726196	4741114	120
			AR-09	2003	725974	4740996	120
		Lobate rock glacier	AR-10	1916	725965	4741185	120
		Upper rock glacier	AR-11	1929	725775	4741244	120
		Moraine	AR-12	1885	725847	4741439	120
Valdeprado	Quartzite (Cabos S.)	Lower rock glacier	VP-01	1556	701733	4753088	120
			VP-02	1569	701681	4753039	120
		Talus slope	VP-03	1672	701594	4752831	120
		Upper rock glacier	VP-04	1732	701386	4752838	120
			VP-05	1735	701364	4752823	120
Vizcodillo	Armorican Quartzite	Millín lowest moraine	VI-01	1560	212539	4677764	120
		Del Lago lowest moraine	VI-02	1614	212408	4677261	120
		Intermediate moraine	VI-03	1802	211789	4676888	120
		Most recent moraine	VI-04	1781	211710	4676805	120
		Talus slope	VI-05	1754	211581	4676616	120
		Polished bedrock	VI-06	1923	211290	4677099	120
		Blockfield	VI-07	2069	210718	4677125	120
			VI-08	2092	210541	4677198	120
			VI-09	2106	210500	4677320	120
San Isidro	Quartzarenite sandstone (Barrios Fm.)	Talus lope	SI-01	1669	306184	4768488	72
		Rock glacier	SI-02	1665	306188	4768504	72
			SI-03	1666	306192	4768514	72
			SI-04	1665	306160	4768526	72
			SI-05	1658	306118	4768555	72
			SI-06	1651	306118	4768586	72
			SI-07	1644	306112	4768598	72
		Lateral ridge	AU-01	1688	308886	4767879	90
		Rock glacier	AU-02	1676	308975	4767830	90
			AU-03	1677	308994	4767804	90
Peña Preita	Granodiorite	Erratics	HP-01	1871	356210	4766366	48
		Moraine	HP-02	2074	357333	4764886	72
			HP-03	2073	357358	4764810	72
		Lower rock glacier	HP-04	2229	357842	4764526	72
			HP-05	2233	357849	4764513	72
		Talus lope	HP-06	2242	357853	4764466	72
			HP-07	2252	357859	4764436	72
		Upper rock glacier	HP-08	2267	357981	4764422	72
		Furrow	HP-09	2264	357990	4764404	72
		Talus slope	HP-10	2278	357996	4764377	72
			HP-11	2290	357999	4764355	72
		Rock outcrop	HP-12	2313	358000	4764320	72

[1] Coordinate system: UTM Zone 29 N, datum ETRS_1989

Table 2. R-values and statics for all sampled sites. SD = standard deviation; CI = 95% confidence interval.

Area	Lithology	Landform	Sample	Mean R-value	Median R-value	SD	CI
Arcos del Agua	Quartzite (Cabos Series)	Lower Rock glacier	AR-01	70.7	71.8	5.2	0.93
			AR-02	72.0	72.0	4.1	0.74
			AR-03	71.7	71.5	4.3	0.78
		Talus slopes	AR-04	74.4	74.5	3.4	0.61
			AR-05	76.2	77.0	3.0	0.54
			AR-06	78.0	78.0	2.4	0.42
			AR-07	77.4	77.5	2.7	0.48
		Blockfield	AR-08	74.9	75.0	3.8	0.68
			AR-09	76.8	77.3	2.6	0.47
		Lobate rock glacier	AR-10	75.0	75.0	3.5	0.62
		Upper rock glacier	AR-11	74.0	73.5	3.5	0.62
		Moraine	AR-12	73.1	73.5	3.8	0.68
Valdeprado	Quartzite (Cabos S.)	Lower rock glacier	VP-01	69.2	70.0	6.4	1.15
			VP-02	65.8	64.5	6.8	1.21
		Talus slope	VP-03	76.6	76.5	2.5	0.44
		Upper rock glacier	VP-04	74.4	75.0	3.7	0.66
			VP-05	75.5	76.0	4.0	0.71
Vizcodillo	Armorican Quartzite	Millín lowest moraine	VI-01	73.8	73.8	4.3	0.77
		Del Lago lowest moraine	VI-02	74.1	74.0	3.0	0.54
		Intermediate moraine	VI-03	75.2	75.0	2.9	0.53
		Most recent moraine	VI-04	76.8	77.0	3.1	0.55
		Talus slope	VI-05	77.3	77.5	2.9	0.52
		Threshold	VI-06	77.5	77.5	2.5	0.78
		Blockfield	VI-07	78.8	79.0	3.0	0.54
			VI-08	79.6	80.0	2.2	0.39
			VI-09	78.8	79.0	2.0	0.36
San Isidro	Quartzarenite sandstone (Barrios Fm.)	Talus lope	SI-01	74.0	74.0	3.9	0.90
		Rock glacier	SI-02	73.5	74.0	5.9	1.37
			SI-03	74.3	75.0	3.8	0.87
			SI-04	73.2	73.0	4.3	0.99
			SI-05	74.0	74.0	4.1	0.95
			SI-06	73.0	73.5	4.3	1.00
			SI-07	73.0	72.8	3.9	0.90
		Lateral ridge	AU-01	63.3	66.5	10.7	2.22
		Rock glacier	AU-02	67.6	69.5	6.3	1.31
			AU-03	69.9	70.8	6.8	1.40
Peña Prieta	Granodiorite	Erratics	HP-01	37.0	39.0	8.1	2.29
		Moraine	HP-02	52.9	53.8	8.0	1.86
			HP-03	57.3	58.0	12.8	2.95
		Lower rock glacier	HP-04	61.0	60.3	7.8	1.81
			HP-05	65.6	68.5	8.7	2.00
		Talus lope	HP-06	67.1	68.0	7.1	1.64
			HP-07	67.9	69.8	7.8	1.80
		Upper rock glacier	HP-08	67.2	70.5	10.1	2.32
		Furrow	HP-09	69.1	70.8	6.5	1.50
		Talus slope	HP-10	70.4	71.0	6.0	1.39
			HP-11	69.2	69.8	6.2	1.43
		Rock outcrop	HP-12	67.8	68.0	7.1	1.64

Figure captions

Figure 1. Location map of the Cantabrian Mountains (SW Europe) and location of the different study areas.

Figure 2. R-values for the five selected study areas. Previous data in Muxivén area (Santos-González et al., 2022a) are also included for reference.

Figure 3. Geomorphological map and mean R-value and SD data in Arcos del Agua.

Figure 4. Mean R-values in the Arcos del Agua area represented on UAV images. A) The Arcos del Agua cirque showing the moraine, upper rock glacier, lobate rock glacier, and blockfields. B) Peña Cefera rock glacier and talus slopes.

Figure 5. Geomorphological map and mean R and SD values in Valdeprado.

Figure 6. A) View of the Busmor rock glacier and talus slope. B) The upper rock glacier and El Miro peak.

Figure 7. Geomorphological map and mean R-value and SD data in Vizcodillo (Del Lago valley).

Figure 8. Sites sampled in the Vizcodillo massif. A) Blockfields around the Vizcodillo peak. B) Blockfield immediately north of the Vizcodillo peak. C) UAV image of the glacial cirque of Lake Truchillas, which shows two distinct moraine stages, a talus slope, and a polished bedrock. D) Moraines in the Millín and Del Lago valleys.

Figure 9. Geomorphological map and R-value and SD data in San Isidro. A) Cebolledo rock glacier. B) Ausente rock glacier.

Figure 10. A) View of the Cebolledo rock glacier and San Isidro ski resort. Note the artificial talus slope generated by a gravel pit in the rock glacier. B) Ausente rock glacier front. C) Detail of sandstone in another rock glacier immediately to the north of the Ausente rock glacier affected by weathering, and no sampled in this work.

Figure 11. Geomorphological map and mean R-value and SD data in Peña Prieta (Hoyo Empedrado valley). The detailed area shows mean R-values and SD for the rock glaciers.

Figure 12. View of the Hoyo Empedrado rock glaciers (Peña Prieta massif), moraines and, in the background, the difluence pass where erratics were sampled.

Figure 13. Different geomorphological stages based on R-value data and geomorphological reconstructions, and probable chronological evolution. Note that SD is not represented in this schematic figure.

Figure 14. Density plot of mean values (a) and standard deviation (b) of R-values by lithological groups.

Declaration of interests

☒The authors declare that they have no known competing financial interests or personal relationships that could have appeared to influence the work reported in this paper.

☐The authors declare the following financial interests/personal relationships which may be considered as potential competing interests:

Graphical abstract

Highlights

- Six stages from the Last Glacial Maximum to the present are inferred
- Relevant differences between R-value and weathering rates depending on lithology
- Paraglacial control rather than climate dependence in the generation of rock glaciers
- Blockfields stabilized after the (almost) total deglaciation of the cirques
- More chronological data are required to construct a proper calibration curve for SHD

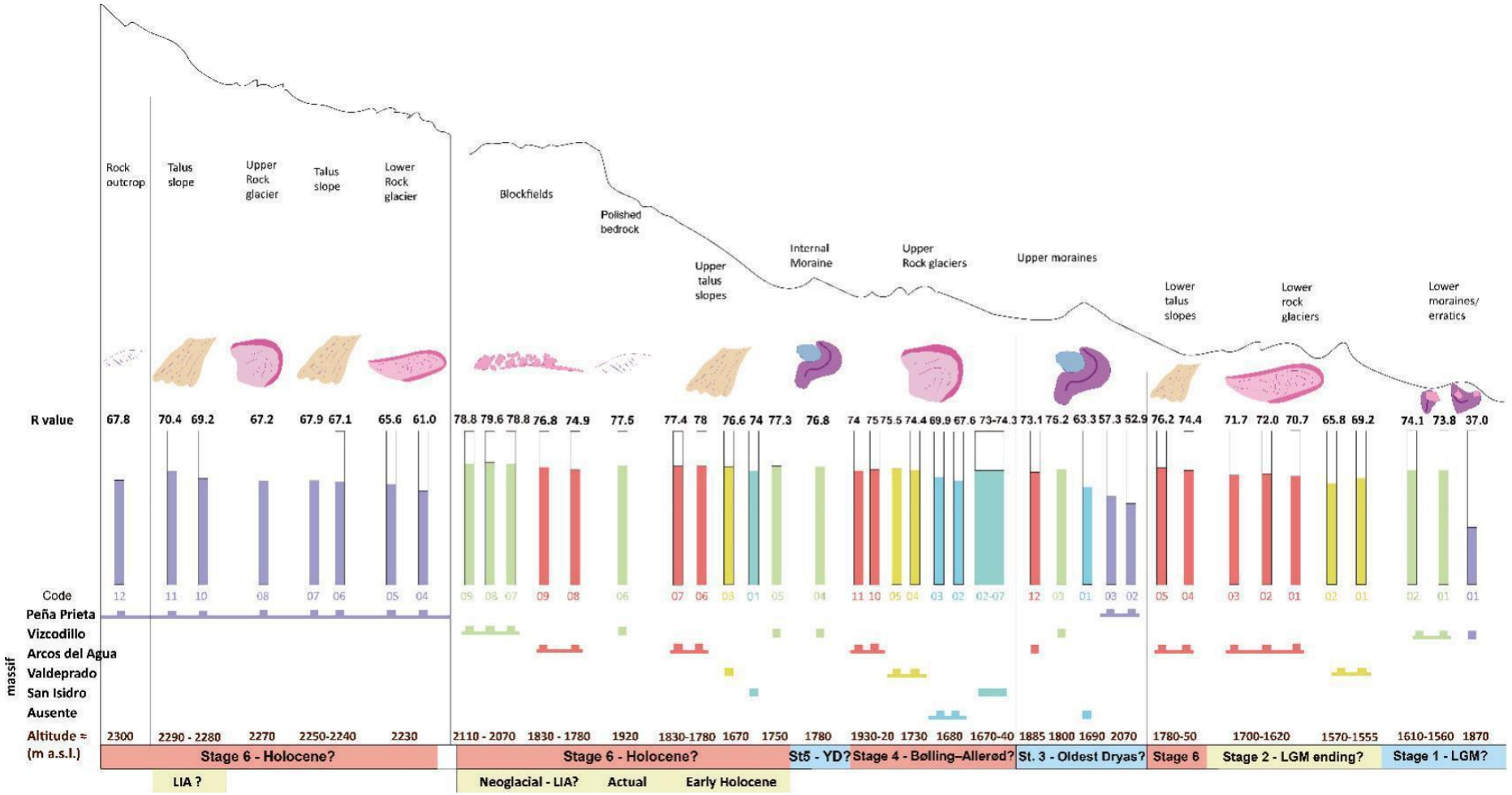

Graphics Abstract

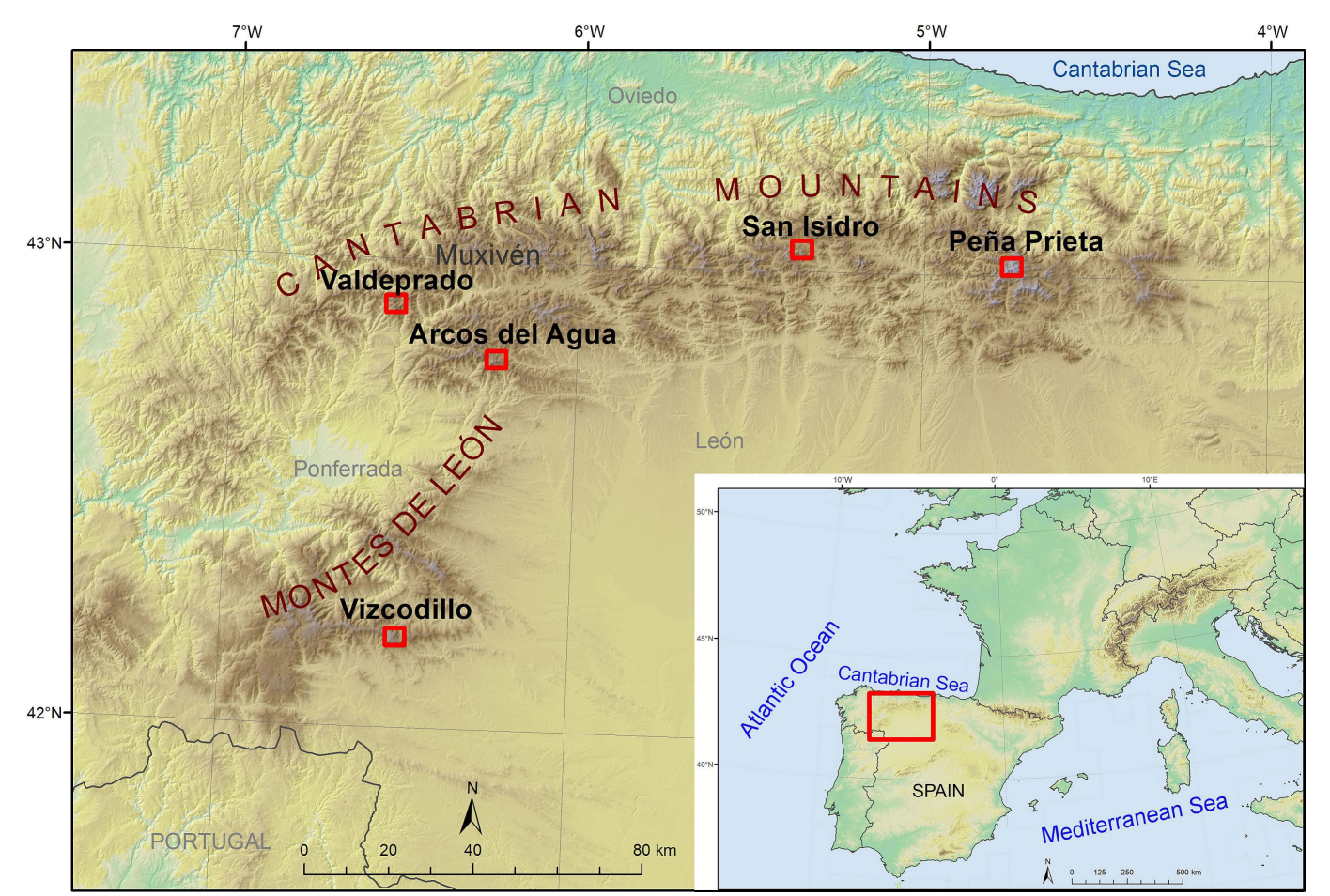
7°W
6°W
5°W
4°W
43°N
42°N
Cantabrian Sea
Oviedo
CANTABRIAN MOUNTAINS
San Isidro
Peña Prieta
Muxivén
Valdeprado
Arcos del Agua
León
Ponferrada
MONTES DE LEÓN
Vizcodillo
PORTUGAL
N
0
20
40
80 km
10°W
0°
10°E
50°N
45°N
40°N
Atlantic Ocean
Cantabrian Sea
SPAIN
Mediterranean Sea
0
125
250
500 km

Figure 1

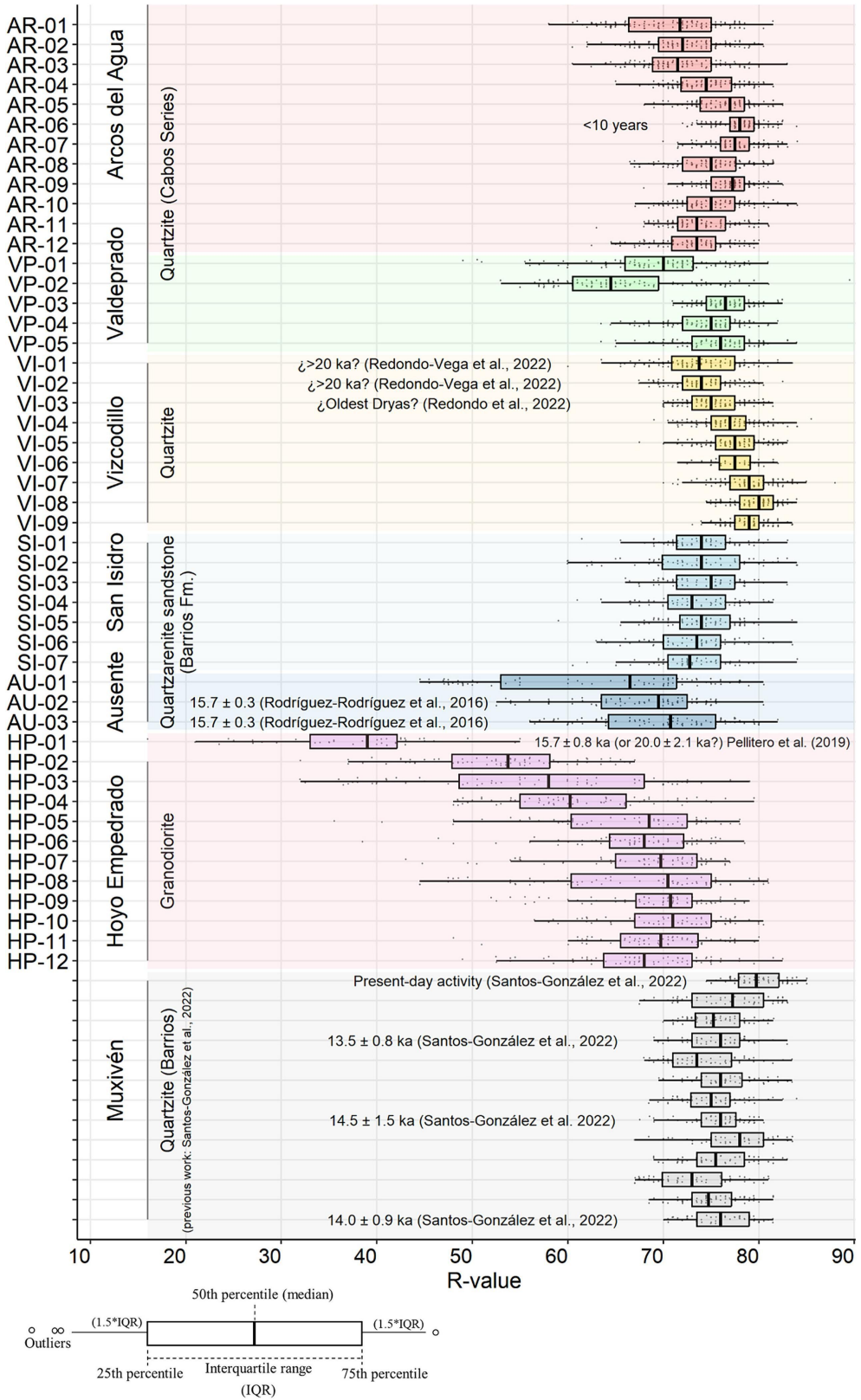
AR-01
AR-02
AR-03
AR-04
AR-05
AR-06
AR-07
AR-08
AR-09
AR-10
AR-11
AR-12
VP-01
VP-02
VP-03
VP-04
VP-05
VI-01
VI-02
VI-03
VI-04
VI-05
VI-06
VI-07
VI-08
VI-09
SI-01
SI-02
SI-03
SI-04
SI-05
SI-06
SI-07
AU-01
AU-02
AU-03
HP-01
HP-02
HP-03
HP-04
HP-05
HP-06
HP-07
HP-08
HP-09
HP-10
HP-11
HP-12
Arcos del Agua
Valdeprado
Vizcodillo
San Isidro
Ausente
Hoyo Empedrado
Muxivén
Quartzite (Cabos Series)
Quartzite
Quartzarenite sandstone (Barrios Fm.)
Granodiorite
Quartzite (Barrios)
(previous work: Santos-González et al., 2022)
<10 years
¿>20 ka? (Redondo-Vega et al., 2022)
¿>20 ka? (Redondo-Vega et al., 2022)
¿Oldest Dryas? (Redondo et al., 2022)
15.7 ± 0.3 (Rodríguez-Rodríguez et al., 2016)
15.7 ± 0.3 (Rodríguez-Rodríguez et al., 2016)
15.7 ± 0.8 ka (or 20.0 ± 2.1 ka?) Pellitero et al. (2019)
Present-day activity (Santos-González et al., 2022)
13.5 ± 0.8 ka (Santos-González et al., 2022)
14.5 ± 1.5 ka (Santos-González et al. 2022)
14.0 ± 0.9 ka (Santos-González et al., 2022)
10
20
30
40
50
60
70
80
90
R-value
50th percentile (median)
(1.5*IQR)
(1.5*IQR)
Outliers
25th percentile
Interquartile range
(IQR)
75th percentile

Figure 2

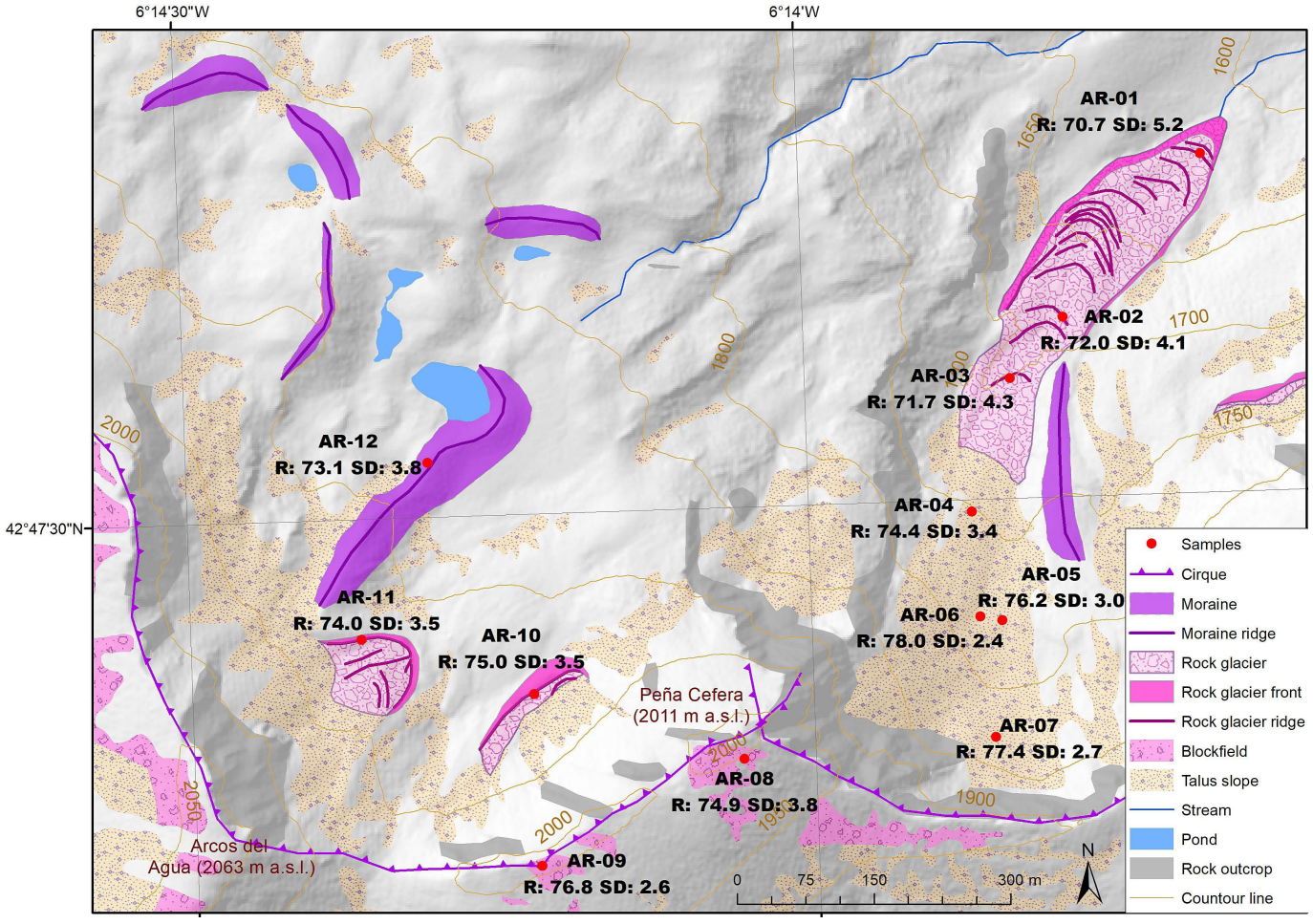
6°14'30"W
6°14'W
42°47'30"N
AR-01
R: 70.7 SD: 5.2
AR-02
R: 72.0 SD: 4.1
AR-03
R: 71.7 SD: 4.3
AR-04
R: 74.4 SD: 3.4
AR-05
R: 76.2 SD: 3.0
AR-06
R: 78.0 SD: 2.4
AR-07
R: 77.4 SD: 2.7
AR-08
R: 74.9 SD: 3.8
AR-09
R: 76.8 SD: 2.6
AR-10
R: 75.0 SD: 3.5
AR-11
R: 74.0 SD: 3.5
AR-12
R: 73.1 SD: 3.8
Peña Cefera
(2011 m a.s.l.)
Arcos del
Agua (2063 m a.s.l.)
1600
1650
1700
1750
1800
1850
1900
1950
2000
2050
Samples
Cirque
Moraine
Moraine ridge
Rock glacier
Rock glacier front
Rock glacier ridge
Blockfield
Talus slope
Stream
Pond
Rock outcrop
Countour line
0
75
150
300 m
N

Figure 3

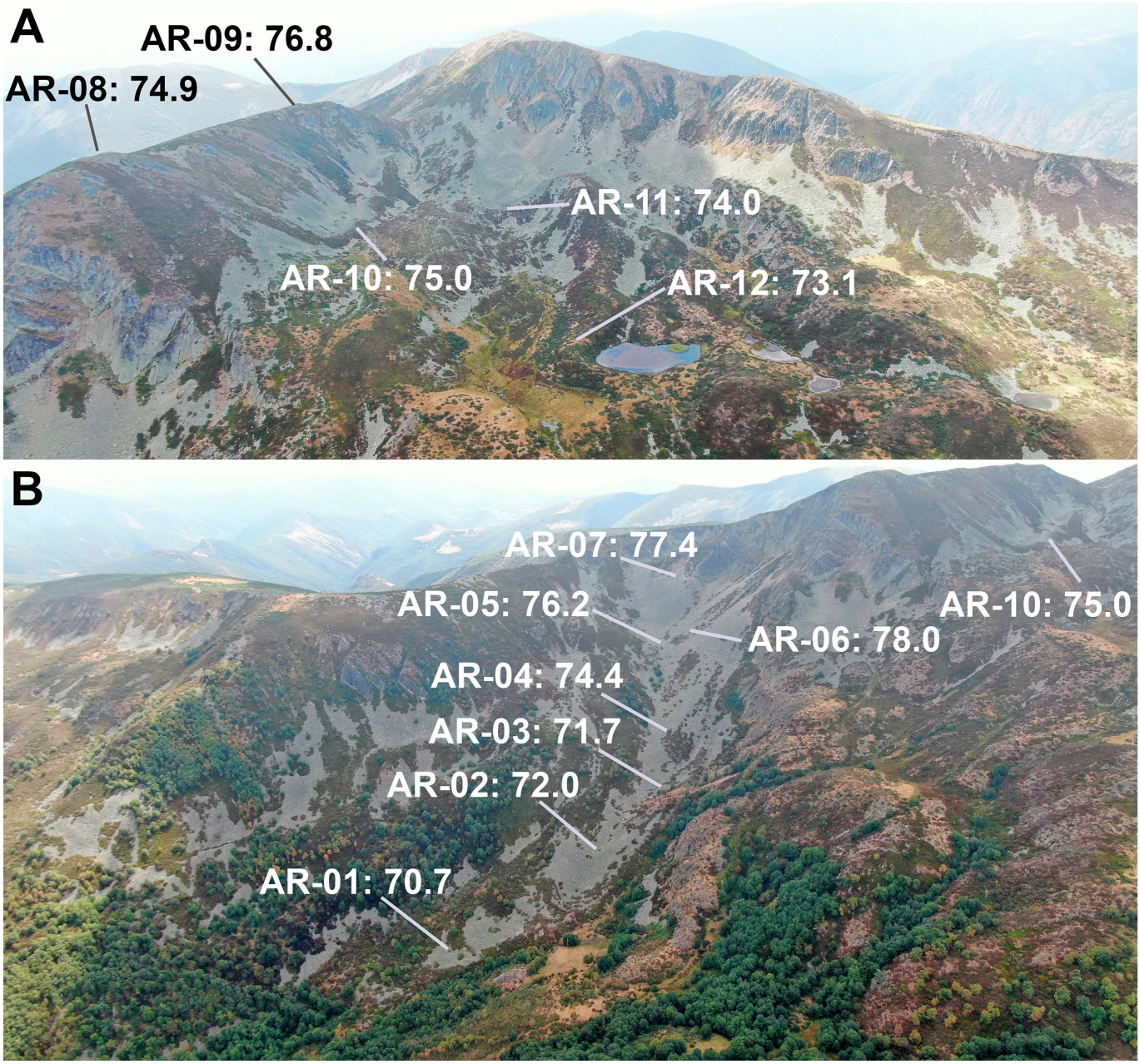
A
AR-09: 76.8
AR-08: 74.9
AR-11: 74.0
AR-10: 75.0
AR-12: 73.1
B
AR-07: 77.4
AR-05: 76.2
AR-10: 75.0
AR-06: 78.0
AR-04: 74.4
AR-03: 71.7
AR-02: 72.0
AR-01: 70.7

Figure 4

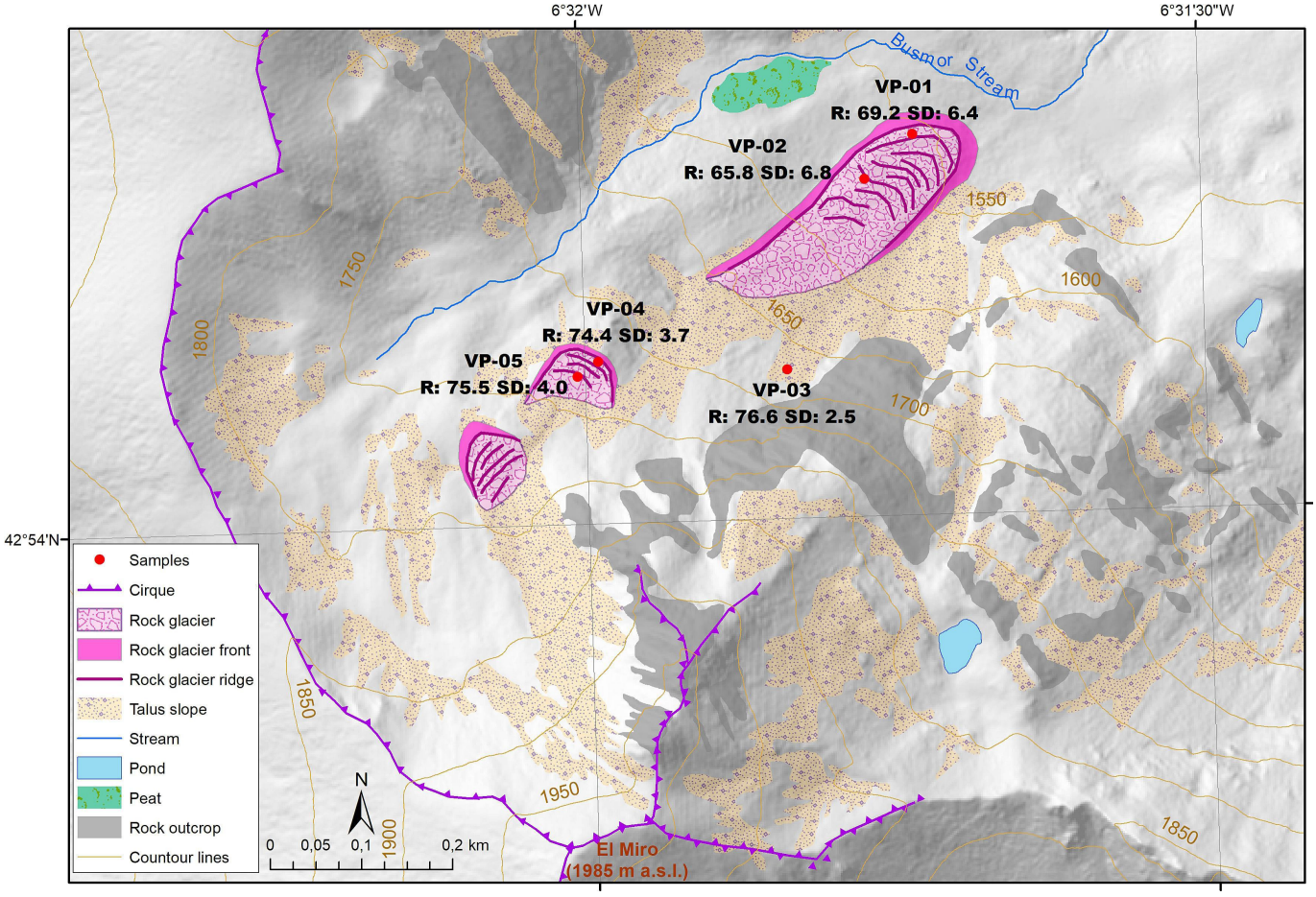
6°32'W
6°31'30"W
42°54'N
Busmor Stream
VP-01
R: 69.2 SD: 6.4
VP-02
R: 65.8 SD: 6.8
VP-04
R: 74.4 SD: 3.7
VP-05
R: 75.5 SD: 4.0
VP-03
R: 76.6 SD: 2.5
1550
1600
1650
1700
1750
1800
1850
1900
1950
Samples
Cirque
Rock glacier
Rock glacier front
Rock glacier ridge
Talus slope
Stream
Pond
Peat
Rock outcrop
Countour lines
N
0
0,05
0,1
0,2 km
El Miro
(1985 m a.s.l.)

Figure 5

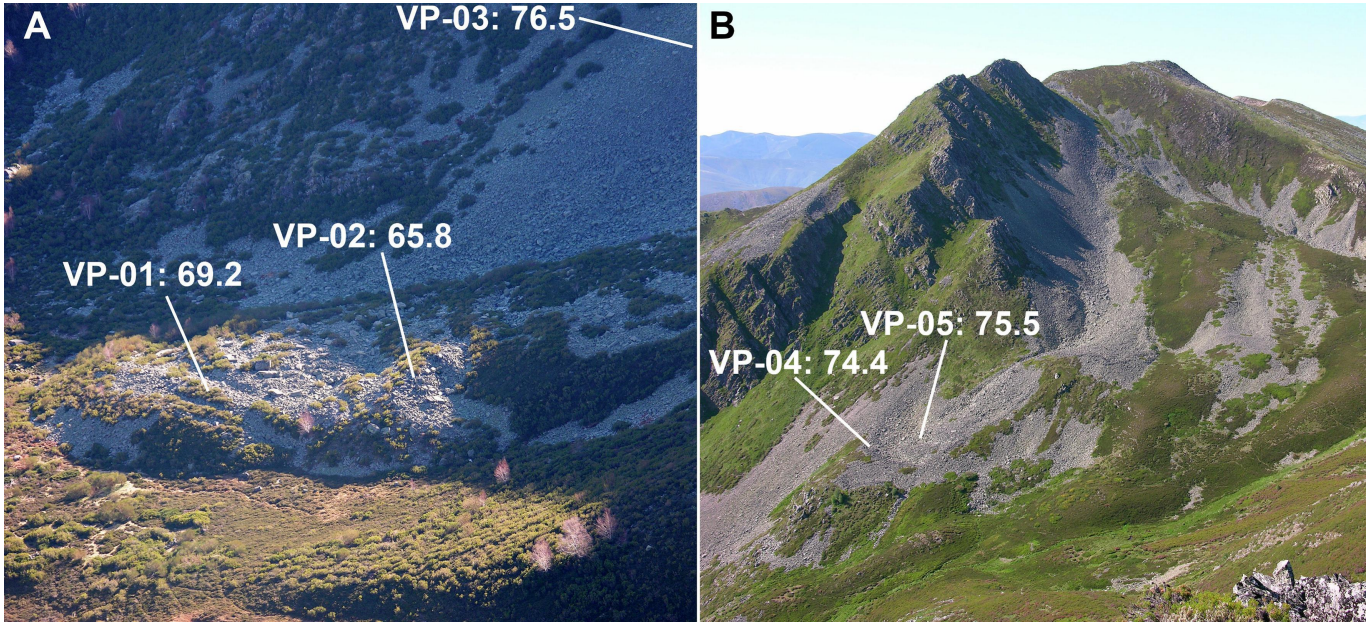

Figure 6

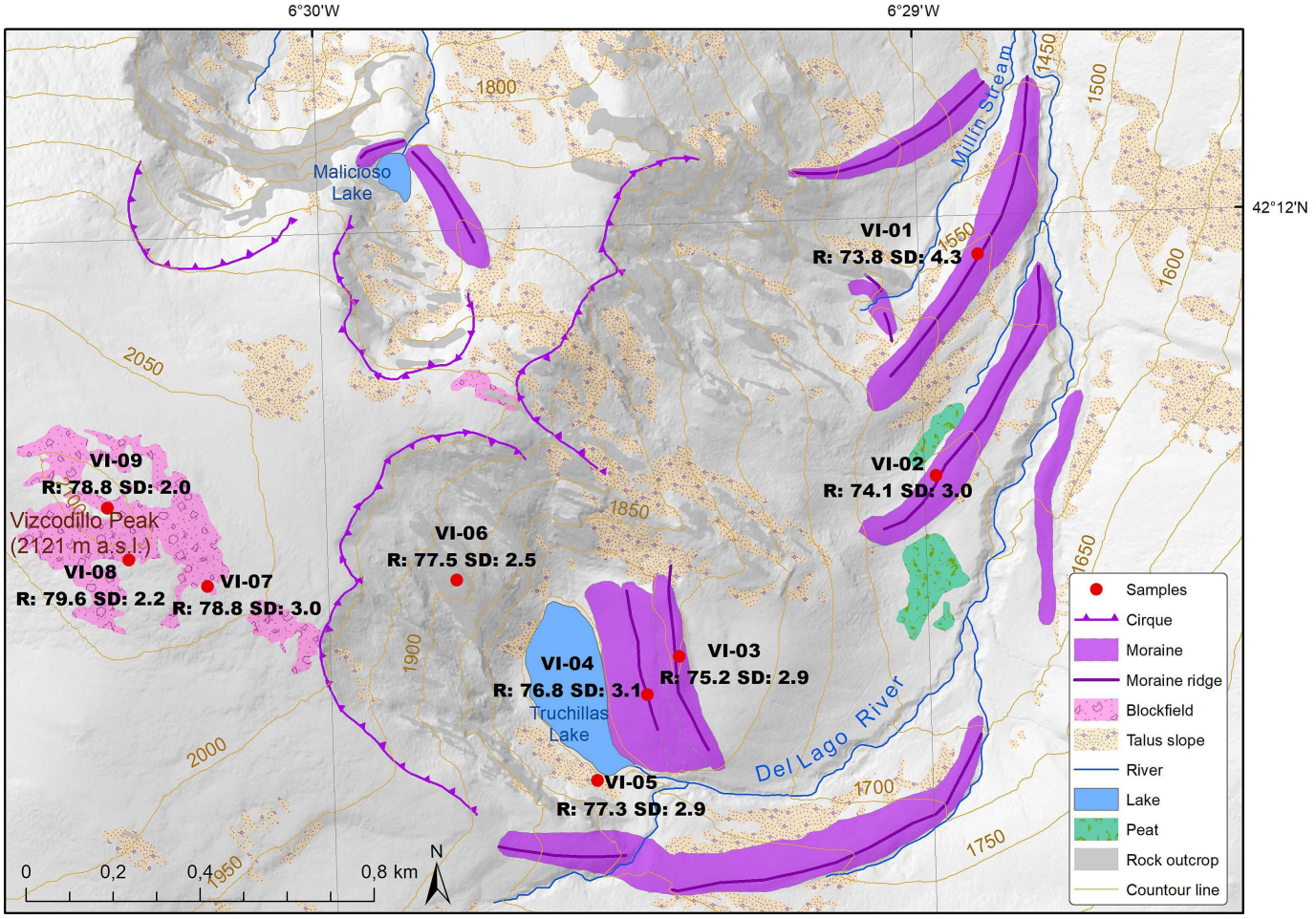
6°30'W
6°29'W
42°12'N
Malicioso Lake
Millín Stream
Vizcodillo Peak (2121 m a.s.l.)
VI-01
R: 73.8 SD: 4.3
VI-02
R: 74.1 SD: 3.0
VI-03
R: 75.2 SD: 2.9
VI-04
R: 76.8 SD: 3.1
VI-05
R: 77.3 SD: 2.9
VI-06
R: 77.5 SD: 2.5
VI-07
R: 78.8 SD: 3.0
VI-08
R: 79.6 SD: 2.2
VI-09
R: 78.8 SD: 2.0
Truchillas Lake
Del Lago River
1450
1500
1550
1600
1650
1700
1750
1800
1850
1900
1950
2000
2050
0
0,2
0,4
0,8 km
N
Samples
Cirque
Moraine
Moraine ridge
Blockfield
Talus slope
River
Lake
Peat
Rock outcrop
Countour line

Figure 7

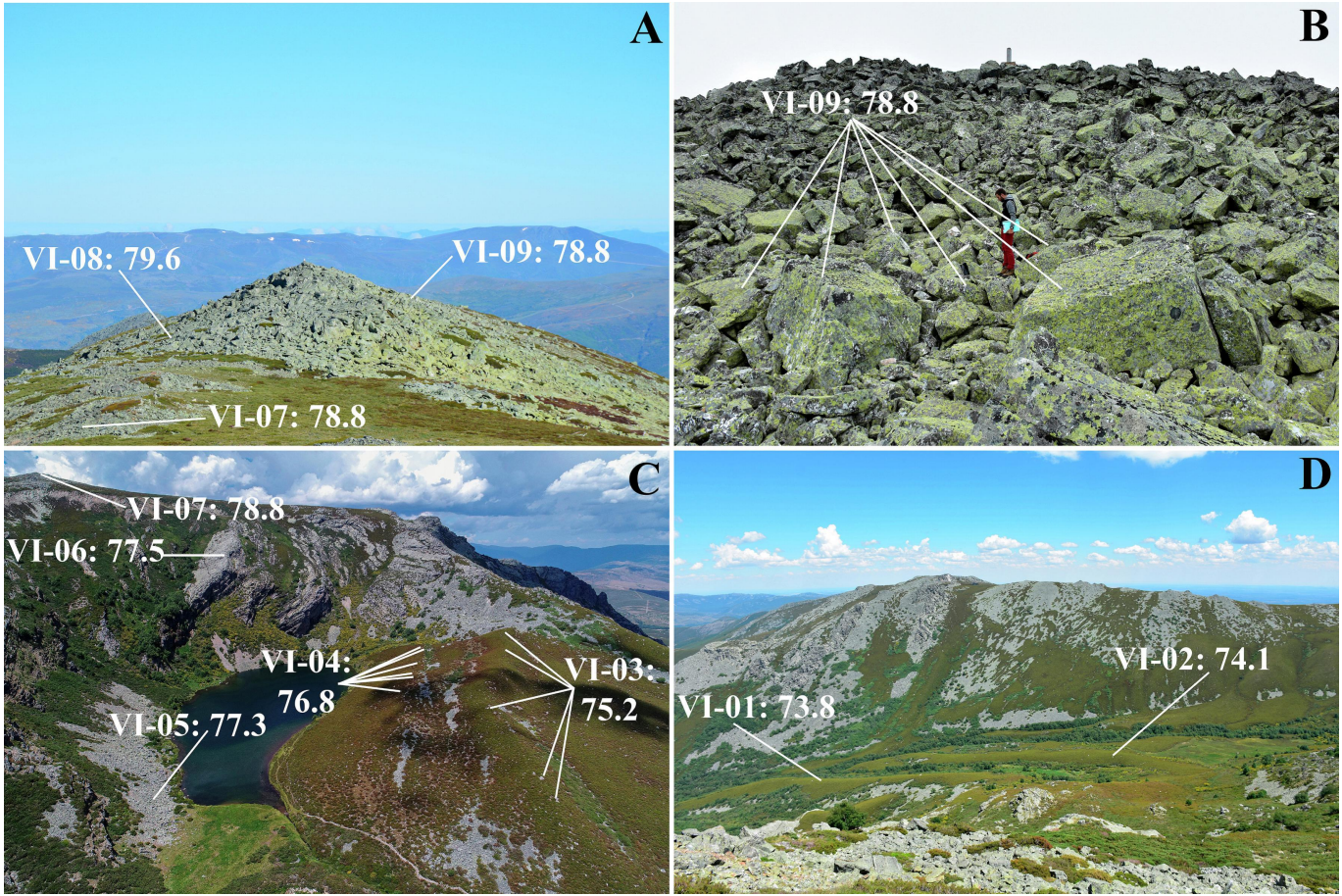
A
VI-08: 79.6
VI-09: 78.8
VI-07: 78.8
B
VI-09: 78.8
C
VI-07: 78.8
VI-06: 77.5
VI-04:
76.8
VI-03:
75.2
VI-05: 77.3
D
VI-02: 74.1
VI-01: 73.8

Figure 8

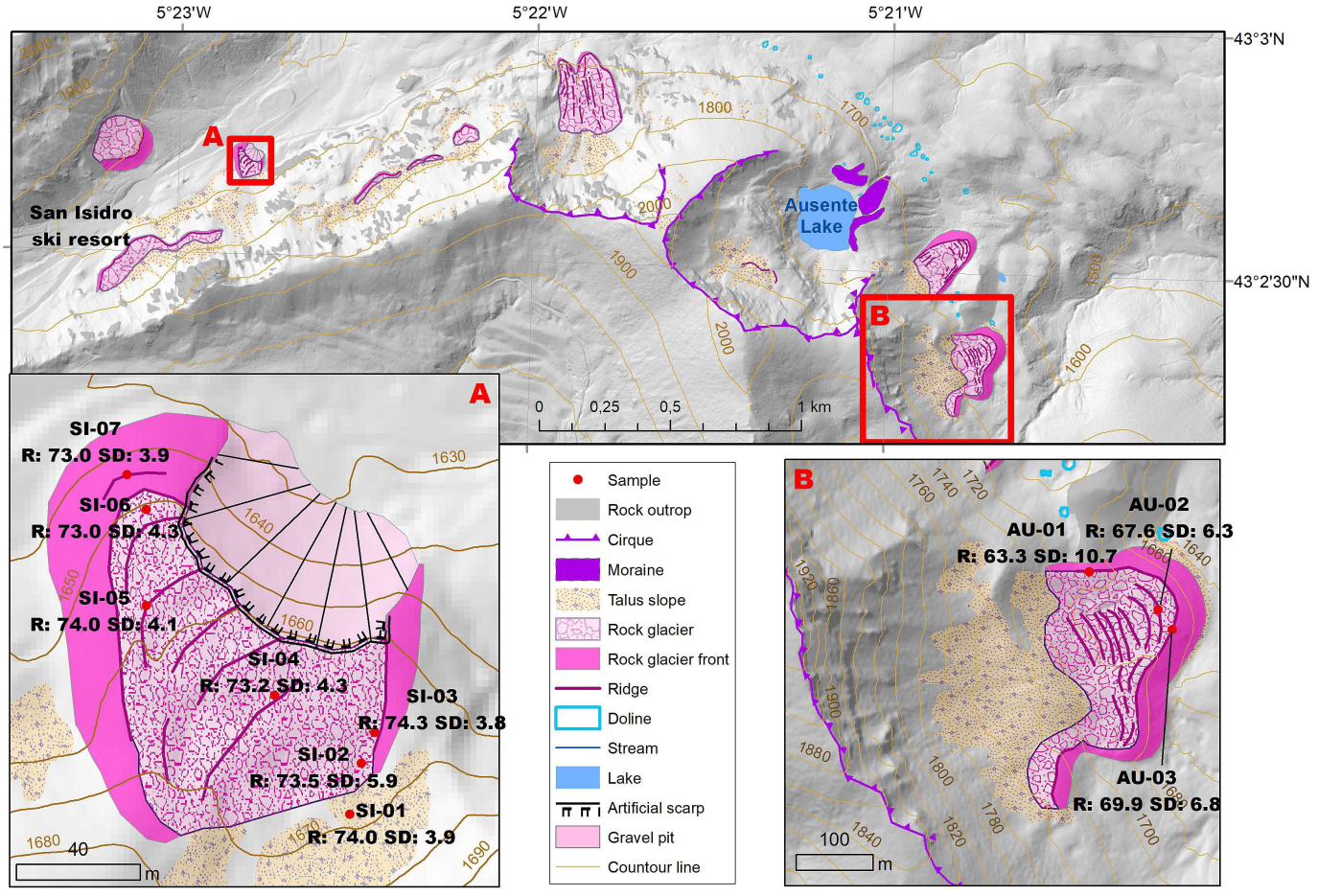
5°23'W
5°22'W
5°21'W
43°3'N
43°2'30"N
San Isidro
ski resort
Ausente
Lake
A
B
0
0,25
0,5
1 km
SI-07
R: 73.0 SD: 3.9
SI-06
R: 73.0 SD: 4.3
SI-05
R: 74.0 SD: 4.1
SI-04
R: 73.2 SD: 4.3
SI-03
R: 74.3 SD: 3.8
SI-02
R: 73.5 SD: 5.9
SI-01
R: 74.0 SD: 3.9
40
m
AU-02
R: 67.6 SD: 6.3
AU-01
R: 63.3 SD: 10.7
AU-03
R: 69.9 SD: 6.8
100
m
Sample
Rock outrop
Cirque
Moraine
Talus slope
Rock glacier
Rock glacier front
Ridge
Doline
Stream
Lake
Artificial scarp
Gravel pit
Countour line

Figure 9

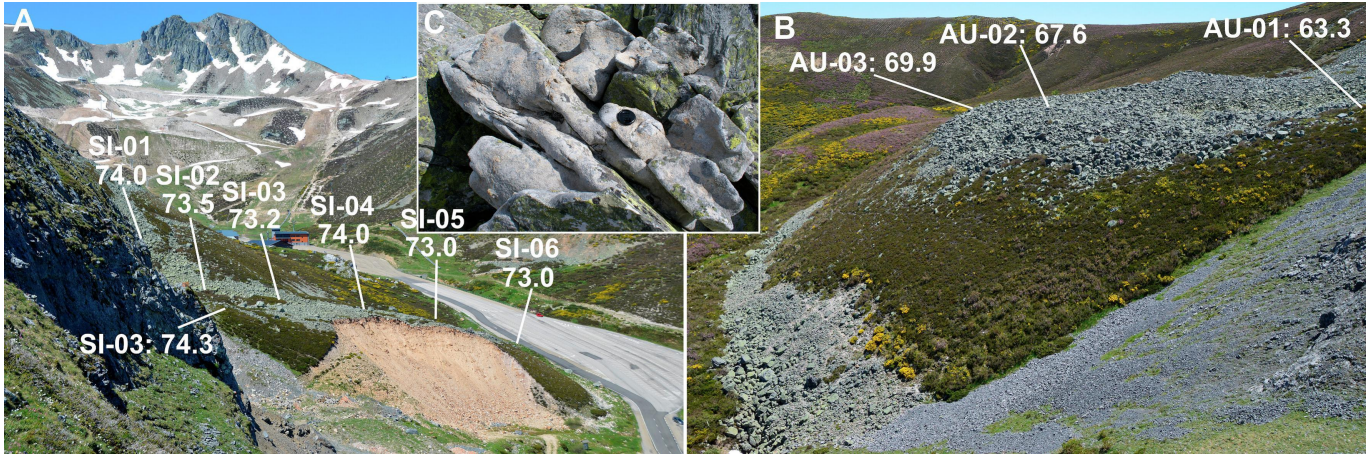
A
SI-01
74.0
SI-02
73.5
SI-03
73.2
SI-04
74.0
SI-05
73.0
SI-06
73.0
SI-03: 74.3
C
B
AU-03: 69.9
AU-02: 67.6
AU-01: 63.3

Figure 10

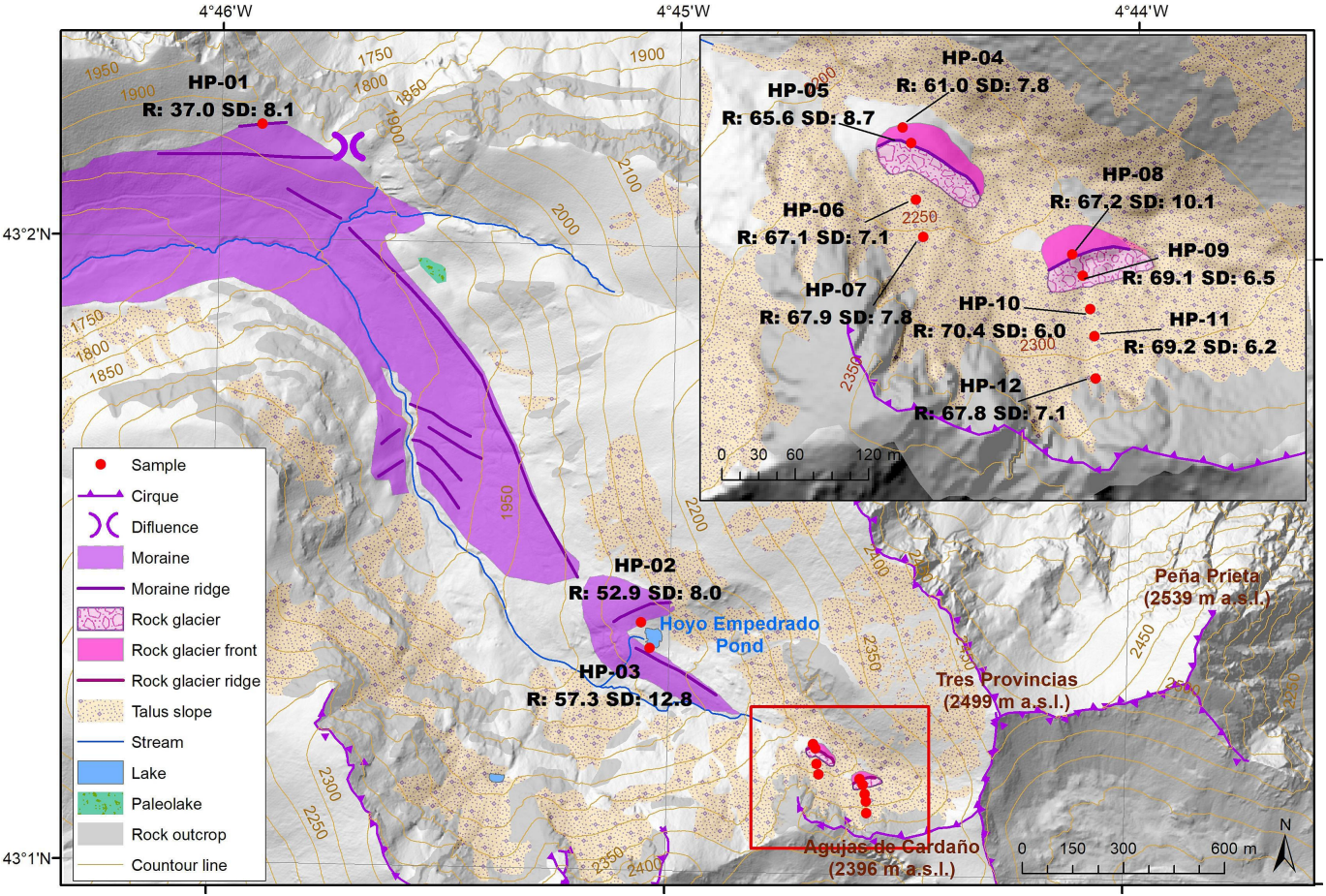
4°46'W
4°45'W
4°44'W
43°2'N
43°1'N
HP-01
R: 37.0 SD: 8.1
HP-02
R: 52.9 SD: 8.0
HP-03
R: 57.3 SD: 12.8
HP-04
R: 61.0 SD: 7.8
HP-05
R: 65.6 SD: 8.7
HP-06
R: 67.1 SD: 7.1
HP-07
R: 67.9 SD: 7.8
HP-08
R: 67.2 SD: 10.1
HP-09
R: 69.1 SD: 6.5
HP-10
R: 70.4 SD: 6.0
HP-11
R: 69.2 SD: 6.2
HP-12
R: 67.8 SD: 7.1
0 30 60 120 m
Hoyo Empedrado
Pond
Peña Prieta
(2539 m a.s.l.)
Tres Provincias
(2499 m a.s.l.)
Agujas de Cardaño
(2396 m a.s.l.)
0 150 300 600 m
N
Sample
Cirque
Difluence
Moraine
Moraine ridge
Rock glacier
Rock glacier front
Rock glacier ridge
Talus slope
Stream
Lake
Paleolake
Rock outcrop
Countour line

Figure 11

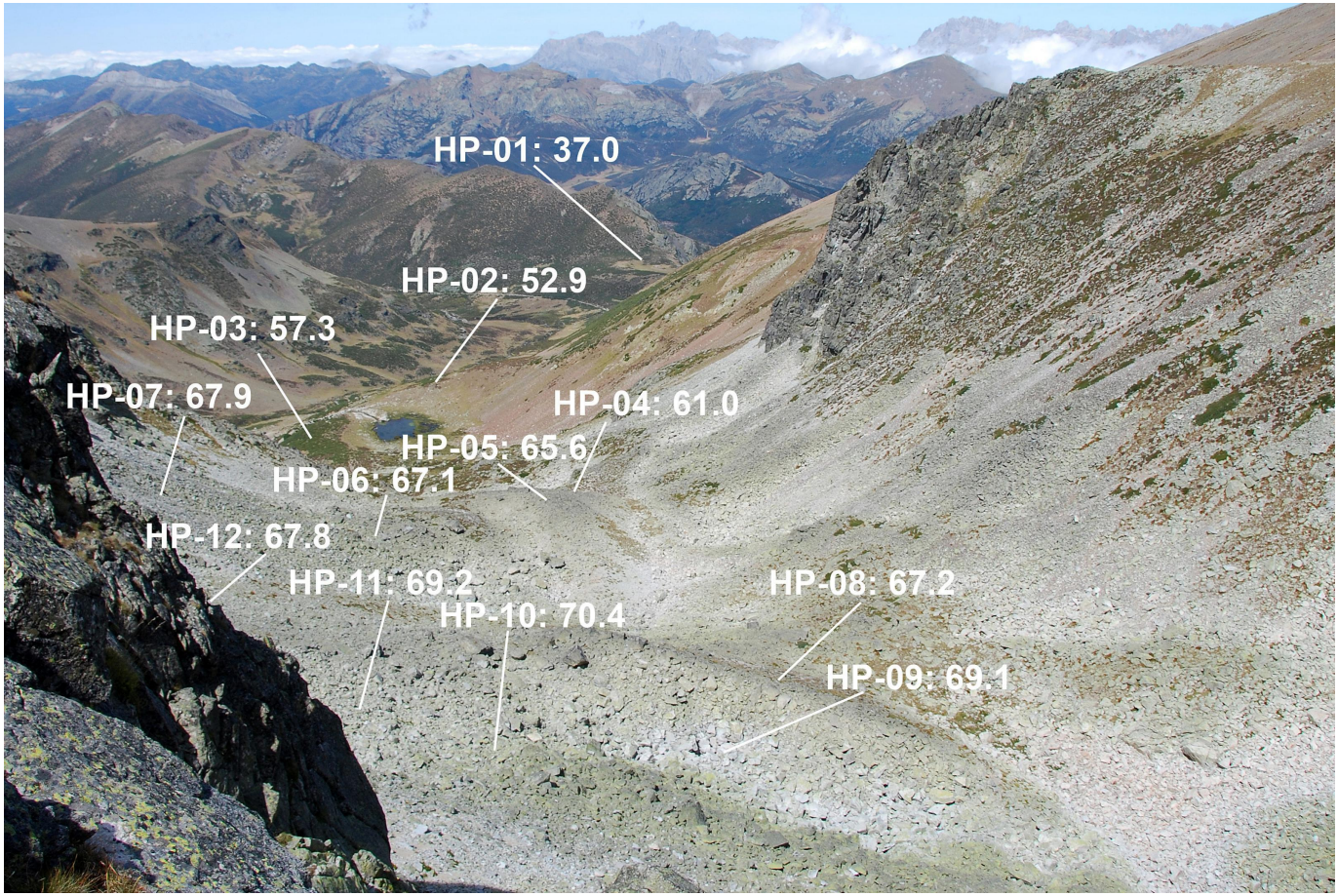
HP-01: 37.0
HP-02: 52.9
HP-03: 57.3
HP-07: 67.9
HP-04: 61.0
HP-05: 65.6
HP-06: 67.1
HP-12: 67.8
HP-11: 69.2
HP-10: 70.4
HP-08: 67.2
HP-09: 69.1

Figure 12

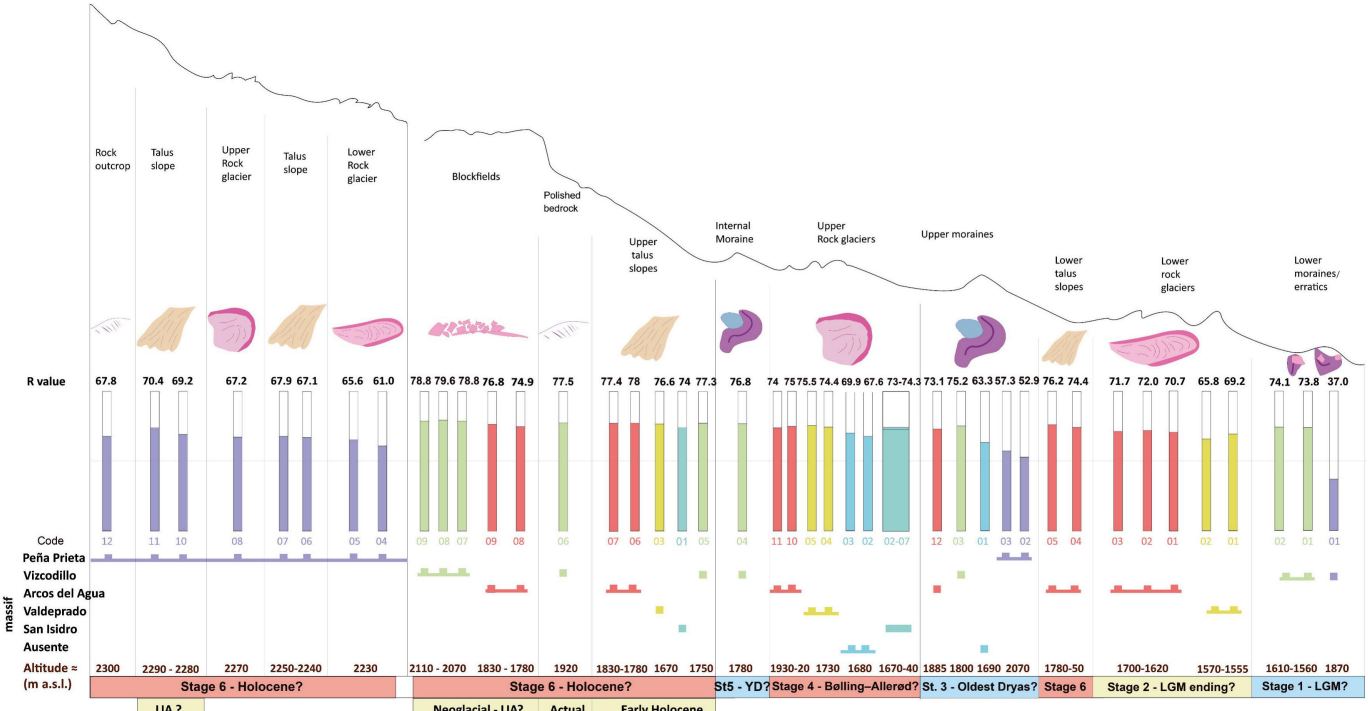
Rock outcrop
Talus slope
Upper Rock glacier
Talus slope
Lower Rock glacier
Blockfields
Polished bedrock
Upper talus slopes
Internal Moraine
Upper Rock glaciers
Upper moraines
Lower talus slopes
Lower rock glaciers
Lower moraines/ erratics
R value
67.8 70.4 69.2 67.2 67.9 67.1 65.6 61.0 78.8 79.6 78.8 76.8 74.9 77.5 77.4 78 76.6 74 77.3 76.8 74 75 75.5 74.4 69.9 67.6 73-74.3 73.1 75.2 63.3 57.3 52.9 76.2 74.4 71.7 72.0 70.7 65.8 69.2 74.1 73.8 37.0
Code
12 11 10 08 07 06 05 04 09 08 07 09 08 06 07 06 03 01 05 04 11 10 05 04 03 02 02-07 12 03 01 03 02 05 04 03 02 01 02 01 02 01 01
massif
Peña Prieta
Vizcodillo
Arcos del Agua
Valdeprado
San Isidro
Ausente
Altitude ≈ (m a.s.l.)
2300 2290 - 2280 2270 2250-2240 2230 2110 - 2070 1830 - 1780 1920 1830-1780 1670 1750 1780 1930-20 1730 1680 1670-40 1885 1800 1690 2070 1780-50 1700-1620 1570-1555 1610-1560 1870
Stage 6 - Holocene?
Stage 6 - Holocene?
St5 - YD?
Stage 4 - Bølling–Allerød?
St. 3 - Oldest Dryas?
Stage 6
Stage 2 - LGM ending?
Stage 1 - LGM?
LIA ?
Neoglacial - LIA?
Actual
Early Holocene

Figure 13

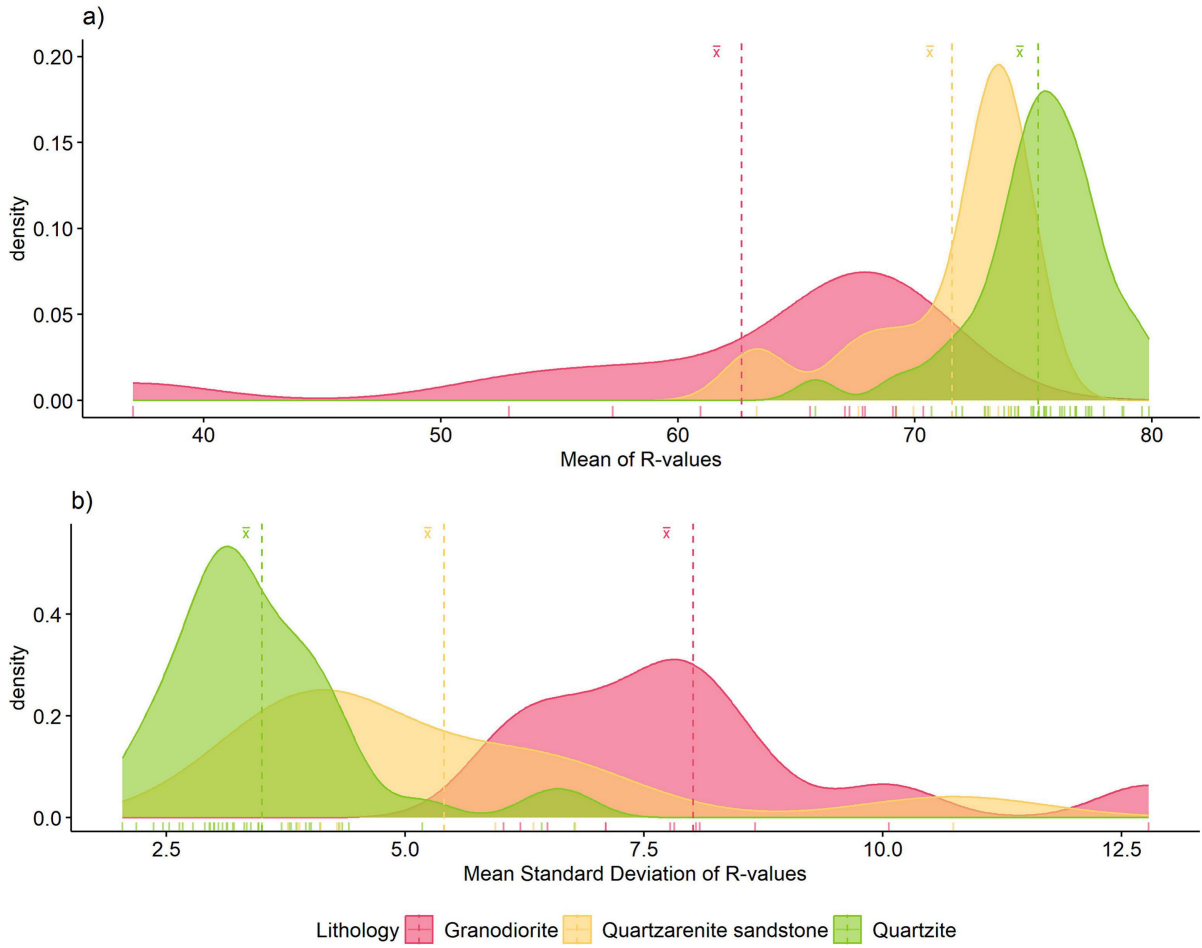
a)
density
0.20
0.15
0.10
0.05
0.00
40
50
60
70
80
Mean of R-values
b)
density
0.4
0.2
0.0
2.5
5.0
7.5
10.0
12.5
Mean Standard Deviation of R-values
Lithology
Granodiorite
Quartzarenite sandstone
Quartzite

Figure 14